PREPARATION AND CHARACTERIZATION OF HEMODIALYSIS MEMBRANES

A Thesis Submitted to
the Graduate School of Engineering and Science of
İzmir Institute of Technology
in Partial Fulfillment of the Requirements for the Degree of

MASTER OF SCIENCE

In Chemical Engineering

by
Filiz YAŞAR MAHLIÇLI

January 2007
İZMİR

We approve the thesis of **Filiz YAŞAR MAHLIÇLI**

Date of Signature

…….. **12 January 2007**

Assoc. Prof. Sacide ALSOY ALTINKAYA

Supervisor

Department of Chemical Engineering

İzmir Institute of Technology

…….. **12 January 2007**

Assoc. Prof. Ahmet YEMENİCİOĞLU

Department of Food Engineering

İzmir Institute of Technology

…….. **12 January 2007**

Assoc. Prof. Oğuz BAYRAKTAR

Department of Environmental Engineering

İzmir Institute of Technology

…….. **12 January 2007**

Prof. Dr. Devrim BALKÖSE

Head of Department

İzmir Institute of Technology

……

Assoc. Prof. Dr. Barış ÖZERDEM

Head of Graduate School

ACKNOWLEDGEMENTS

First, I would like to present my deepest thanks to my supervisor Associate Professor Sacide Alsoy Altınkaya who made this study possible with her support, guidance, encouragment and understanding.

I would like to thank to Associate Professor Ahmet Yemenicioğlu who has shared his knowledge and experience whenever I needed.

I also would like to thank to my friends Senem Yetgin, Seyhun Gemili, Şeniz Yılmaz, Cem Göl, İlker Polatoğlu, Ali Emrah Çetin, Cihan Çiftlikli and Özge Aslan for their helps and encouragements.

I would like to appreciate deeply to my family for their endless understanding and love.

Finally, I would like to express my hearty gratitude to my dear husband Berkan Mahlıçlı for being with me in every situation.

ABSTRACT

PREPARATION AND CHARACTERIZATION OF HEMODIALYSIS MEMBRANES

Hemodialysis is a widely used clinical therapy for end-stage renal failure and dialysis membranes are vital components of a hemodialysis unit. The most desirable properties of a hemodialysis membrane are high mass transfer of toxic solutes to reduce the dialysis time, blood compatibility and limited protein adsorption capacity. Protein adsorption or deposition on the surface or in its pores results in a progressive decline in flux, change of selectivity of the membrane and the activation of different defense systems in blood. To prepare hemodialysis membranes with improved transport properties and protein adsorption resistant surfaces, an enzyme immobilization technique was used. Asymmetric cellulose acetate membranes were prepared through dry phase inversion method and they were modified by blending urease enzyme directly into the casting solution. The effect of enzyme immobilization on the protein adsorption, solute transport rates and mechanical properties was investigated through static adsorption and permeation experiments, mechanical tests and structural characterization by scanning electron microscope. It was found that the solute permeation rates decreased exponentially while the maximum tensile strength of the membranes increased significantly by increasing the cellulose acetate (CA) to acetone weight fraction ratio in the membrane forming solution due to a change in the structure from porous to dense one. Modification of the CA membrane with urease immobilization increased the permeation coefficients of creatinine and uric acid by a factor of 1.2 and 1.7, respectively. Similarly, the % removal of urea from the donor compartment in 1 hour increased from 45.8% to 53.2% by using urease immobilized CA membrane. The protein adsorption capacity of the urease immobilized CA membrane was found to be 2 times lower than that of the regular CA membrane. Protein fouling on the membranes caused a decrease in the transport rates of all solutes. Due to protein fouling, the decrease in the permeation coefficients of creatinine and uric acid are 59.0% and 76.5%, respectively, through regular CA membranes. On the other hand, urease immobilization limited the decrease in the permeation rates by 39.2% and 33.4% for creatinine and uric acid, respectively. In a similar way, the rate of removal of urea through CA membrane and urease immobilized CA membrane decreased by 31.2% and 11.7%, respectively. While urease immobilization decreased the protein adsorption capacity, it did not cause any loss in mechanical strength of the membrane. These results indicate that urease immobilization can be used to improve transport properties and reduce protein adsorption capacity of the CA membranes. Urease immobilized CA membranes prepared in this study can be used as an alternative membrane in hemodialysis units.

ÖZET

HEMODİYALİZ ZARLARININ HAZIRLANMASI VE KARAKTERİZASYONU

Hemodiyaliz, böbrek yetmezliği hastalığında en sık kullanılan tedavi yöntemidir ve diyaliz membranı hemodiyaliz ünitesinin en önemli parçasıdır. Bir hemodiyaliz membranından beklenen; diyaliz süresini kısaltmak için toksik bileşenlere karşı yüksek geçirgenliğe, kan uyumluluğuna ve düşük protein adsorpsiyon kapasitesine sahip olmasıdır. Membran yüzeyinde ve gözeneklerinde proteinlerin birikmesi, membrandan geçiş hızının zamanla yavaşlayarak ayırma işlemi için gerekli olan sürenin uzamasına, seçiciliğin değişmesine ve kandaki diğer bileşenlerle istenmeyen reaksiyonların oluşumuna sebep olur. Bu çalışmada, iyileştirilmiş geçiş özelliklerine sahip ve protein adsorpsiyonuna karşı dirençli membranlar hazırlamak için enzim immobilizasyon tekniği kullanılmıştır. Asimetrik selüloz asetat membranları faz ayrımı yöntemi ile hazırlanmış ve membran çözeltisi ile üreaz enzimi harmanlanarak modifiye edilmiştir. Enzim immobilizasyonunun protein adsorpsiyonu, bileşenlerin geçiş hızları ve mekanik özellikleri üzerindeki etkisi; statik adsorpsiyon ve geçirgenlik deneyleri, mekanik dayanım testi ile ve taramalı elektron mikroskobu ile yapısal özelliklerine bakılarak tespit edilmiştir. Membran çözeltisi içerisindeki selüloz asetat/aseton oranı artırıldığında membranın gözenekli bir yapıdan daha yoğun bir yapıya dönüştüğü; mekanik dayanıklılığının arttığı ve geçiş hızlarının azaldığı bulunmuştur. CA membranının üreaz ile modifikasyonu kreatin ve ürik asitin geçirgenlik katsayılarını sırası ile 1.2 ve 1.7 kat artırmıştır. Benzer bir şekilde, üreaz immobilize edilmiş CA membranından ürenin 1 saat içerisindeki % uzaklaşma hızı % 45.8' den % 53.2' ye yükselmiştir. Üreaz immobilize edilmiş CA membranının protein adsorpsiyon kapasitesi CA membranınınkinden 2 kat daha düşük olarak bulunmuştur. Membranların protein ile kirlenmesi tüm bileşenlerin geçiş hızlarında azalmaya sebep olmaktadır. Membranın protein ile kirlenmesi sonucu, kreatin ve ürik asitin CA membranından geçiş hızlarındaki azalma sırası ile % 59.0 ve % 76.5' dir. Diğer taraftan, üreaz immobilizasyonu kreatin ve ürik asitin geçiş hızlarındaki azalmayı % 39.2 ve % 33.4' e düşürmüştür. Benzer bir yolla, ürenin üreaz immobilize edilmiş CA membranından uzaklaşma hızındaki azalma % 31.2' den % 11.7' ye düşmüştür. Üreaz immobilizasyonu protein adsorpsiyon kapasitesini azaltırken, mekanik özelliklerde herhangi bir azalmaya neden olmamıştır. Bu sonuçlar üreaz immobilizasyon tekniğinin CA membranlarının geçiş özelliklerini iyileştirmede ve protein adsorpsiyon kapasitelerini azaltmada kullanılabilecek bir yöntem olduğunu göstermektedir. Bu çalışmada hazırlanan üreaz immobilize edilmiş CA membranları hemodiyaliz ünitelerinde alternatif bir membran olarak kullanılabilir.

TABLE OF CONTENTS

LIST OF FIGURES ix
LIST OF TABLES xiii

CHAPTER 1. INTRODUCTION 1

CHAPTER 2. HEMODIALYSIS OPERATION 3
2.1. Types of Modules 5
2.2. Types of Membranes 6
2.2.1. Unmodified Cellulosic Membrane 6
2.2.2. Modified Cellulosic Membrane 6
2.2.3. Synthetic Membrane 7
2.3. Properties of Hemodialysis Membranes 8
2.4. Characterization Tools for Hemodialysis Membranes 9

CHAPTER 3. PHASE INVERSION TECHNIQUE 11
3.1. Thermally Induced Phase Separation 11
3.2. Nonsolvent (Vapor) Induced Phase Separation 13
3.3. Wet Phase Inversion Method 13
3.4. Dry Phase Inversion 14

CHAPTER 4. PROTEIN FOULING ON MEMBRANES 16
4.1. Using Asymmetric Membrane 16
4.2. Cleaning and Regeneration of Membranes 17
4.2.1. Physical Methods 17
4.2.1.1. Backflushing 17
4.2.1.2. Periodic Reversal of the Feed Stream 17
4.2.2. Chemical Cleaning 17
4.3. Modification of Membrane Surfaces for Antifouling 18
4.3.1. Introduction of Negatively Charged Surface Groups 18
4.3.2. Increasing Hydrophilicity 21
4.3.2.1. Physical Coating 22

4.3.2.2. Blending 23
4.3.2.3. Chemical Modification 26
4.3.2.4. Photochemical Modification 27
4.3.2.5. Irradiation 27
4.3.2.6. Plasma Polymerization 27
4.3.3. Introduction of Steric Hindrance 27
4.3.3.1. Irreversible Adsorption 28
4.3.3.2. Chemical Grafting 28
4.3.4. Biomimetic Modifications 29

CHAPTER 5. TRANSPORT OF SOLUTES THROUGH HEMODIALYSIS MEMBRANES 30
5.1. Transport of Solutes Through Noncatalytic Membranes 30
5.2. Transport of Solutes Through Catalytic Membrane 33

CHAPTER 6. EXPERIMENTAL STUDIES 36
6.1. Materials 36
6.2. Preparation of Membranes 36
6.3. Protein Adsorption Experiments 37
6.4. Determination of immobilized urease activity 37
6.4.1. Determination of Immobilized Urease Stability in Buffer 39
6.4.2. Determination of Immobilized Urease Stability in Dry Membrane 39
6.5. Permeation Experiments 39
6.6. Characterization Studies 41
6.6.1. Measurement of Tensile Strength 41
6.6.2. Surface Characterization 42

CHAPTER 7. RESULTS AND DISCUSSION 43
7.1. Influence of Polymer Concentration on the Permeation of Solutes Through CA Membranes 43
7.2. Characterization of Urease Immobilized Cellulose Acetate Membranes 52
7.2.1. Determination of Stability of Immobilized Urease Activities 52

7.2.2. Determination of Kinetic Parameters of Immobilized Urease 53
7.3. Permeation of Solutes Through Urease Immobilized Cellulose Acetate Membranes 55
7.4. Permeation of Solutes Through Protein Fouled Cellulose Acetate Membranes 61
7.5. Mechanical Properties of Cellulose Acetate Membranes 69

CHAPTER 8. COCLUSIONS AND RECOMMENDATIONS FOR FUTURE WORK 75

REFERENCES 77

APPENDIX A. CALIBRATION CURVES 81

LIST OF FIGURES

Figure **Page**

Figure 2.1. Typical Hemodialysis System 3

Figure 3.1. Idealized solid-liquid (S/L) TIPS phase diagram that incorporates the effect of cooling rate on crystallization to distinguish equilibrium and pseudoequlibrium conditions 12

Figure 3.2. Cross section morphology of cellulose acetate membrane prepared by wet phase inversion method 14

Figure 3.3. Concentration paths of water, acetone and cellulose acetate solution: (○) solution/air interface; (□): solution/substrate interface..... 15

Figure 4.1. Schematic diagram of the filtration behavior of (a) an asymmetric and (b) a symmetric membrane..... 16

Figure 4.2. Comparison of platelet adhesion on membranes after 30 min, 1 and 2 h incubation..... 20

Figure 4.3. Comparison of thrombus formation on membranes after 30 min, 1 h and 2 h incubation 21

Figure 4.4. Permeation coefficient for cytochrome C through the asymmetric porous membranes before (white bar) and after (black bar) contact with protein solution..... 24

Figure 4.5. Adsorption pattern of plasma proteins on CA and CA/PMB30 blend membrane surfaces after contact with human plasma for 90 min 25

Figure 4.6. Amount of proteins adsorbed on CA (hatched bar) and CA/ PMB30 (black bar) and polysulfone (white bar) membranes..... 26

Figure 5.1. Schematic diagram of a diffusion cell 30

Figure 6.1. Experimental set-up used for permeation experiments..... 40

Figure 7.1. The change of $ln\frac{C_D - C_R}{C_{Di} - C_{Ri}}$ with respect to time for the permeation of urea through CAI membrane 44

Figure 7.2. The change of $ln\frac{C_D - C_R}{C_{Di} - C_{Ri}}$ with respect to time for the permeation of uric acid through CAI membrane. 44

Figure 7.3. The change of $ln\frac{C_D - C_R}{C_{Di} - C_{Ri}}$ with respect to time for the permeation of creatinine through CAI membrane. 45

Figure 7.4. The change of $ln\frac{C_D - C_R}{C_{Di} - C_{Ri}}$ with respect to time for the permeation of urea through CAII membrane. 45

Figure 7.5. The change of $ln\frac{C_D - C_R}{C_{Di} - C_{Ri}}$ with respect to time for the permeation of uric acid through CAII membrane. 46

Figure 7.6. The change of $ln\frac{C_D - C_R}{C_{Di} - C_{Ri}}$ with respect to time for the permeation of creatinine through CAII membrane. 46

Figure 7.7. The change of $ln\frac{C_D - C_R}{C_{Di} - C_{Ri}}$ with respect to time for the permeation of urea through CAIII membrane. 47

Figure 7.8. The change of $ln\frac{C_D - C_R}{C_{Di} - C_{Ri}}$ with respect to time for the permeation of uric acid through CAIII membrane. 47

Figure 7.9. The change of $ln\frac{C_D - C_R}{C_{Di} - C_{Ri}}$ with respect to time for the permeation of creatinine through CAIII membrane. 48

Figure 7.10. The permeation coefficients of three model solutes through CAI, CAII and CAIII membranes. 49

Figure 7.11. SEM picture of CAI membrane, magnification 1000x 50

Figure 7.12. SEM picture of CAII membrane, magnification 2500x 50

Figure 7.13. SEM picture of CAIII membrane, magnification 5000x 51

Figure 7.14. The effect of storing time on the relative activity of urease immobilized in CAI membrane. Initial activity of urease=1.18 micromole NH_3 / min x cm². Membrane was stored in phosphate buffer solution at pH=7.4, T=37°C 52

Figure 7.15. The effect of storing time on the relative activity of urease immobilized in CAI membrane. Initial activity of urease=1.18 micromol NH_3 / min x cm². Membrane was stored in dry form at 4°C. 53
Figure 7.16. Kinetic parameters of urease immobilized CA membrane. 54
Figure 7.17. The change of $ln\frac{C_D - C_R}{C_{Di} - C_{Ri}}$ with respect to time for the permeation of uric acid through urease immobilized CA membrane..... 55
Figure 7.18. The change of $ln\frac{C_D - C_R}{C_{Di} - C_{Ri}}$ with respect to time for the permeation of creatinine through urease immobilized CA membrane..... 56
Figure 7.19. SEM picture of urease immobilized CA membrane, magnification 5000x 57
Figure 7.20. The change of concentration of urea in a) donor b) receiver compartments with respect to time when regular CA and urease immobilized CA membranes were used. 58
Figure 7.21. Comparison of model predictions with the experimental data for the concentration of urea in both donor and receiver compartments. 59
Figure 7.22. Predictions of concentration of urea in the donor compartment. Model 1 gives the urea concentration when regular CA membrane is used, while model 2 predicts the urea concentration when urease immobilized CA membrane is used. 60
Figure 7.23. Amount of BSA adsorbed on cellulose acetate and urease immobilized cellulose acetate membranes. 62
Figure 7.24. The change of $ln\frac{C_D - C_R}{C_{Di} - C_{Ri}}$ with respect to time for the permeation of uric acid through BSA fouled CAI membrane. 63
Figure 7.25. The change of $ln\frac{C_D - C_R}{C_{Di} - C_{Ri}}$ with respect to time for the permeation of creatinine through BSA fouled CAI membrane. 63

Figure 7.26. The change of $ln\frac{C_D - C_R}{C_{Di} - C_{Ri}}$ with respect to time for the permeation of uric acid through BSA fouled urease immobilized CA membrane. 64
Figure 7.27. The change of $ln\frac{C_D - C_R}{C_{Di} - C_{Ri}}$ with respect to time for the permeation of creatinine through BSA fouled urease immobilized CA membrane. 64
Figure 7.28. The change of permeation coefficient of uric acid due to protein fouling on CAI and urease immobilized CA membranes. 65
Figure 7.29. The change of permeation coefficient of creatinine due to protein fouling on CAI and urease immobilized CA membranes. 65
Figure 7.30. The change of concentration of urea in a) donor b) receiver compartments with respect to time when BSA fouled regular CA and urease immobilized CA membranes were used 66
Figure 7.31. The change of % removal of urea due to protein fouling on CAI and urease immobilized CA membranes. 67
Figure 7.32. Comparison of model predictions with the experimental data for the concentration of urea in both donor and receiver compartments. 67
Figure 7.33. Predictions of concentration of urea in the donor compartment. Model 1 gives the urea concentration when BSA fouled regular CA membrane is used, while model 2 predicts the urea concentration when BSA fouled urease immobilized CA membrane is used. 68
Figure 7.34. Stress vs. strain curve for CAI membrane. 69
Figure 7.35. Stress vs. strain curve for CAII membrane 70
Figure 7.36. Sress vs. strain curve for CAIII membrane. 70
Figure 7.37. Stress vs. strain curve for urease immobilized CA membrane 71

LIST OF TABLES

Table **Page**

Table 4.1. Plasma protein adsorption onto the PAN membrane 19

Table 7.1. Compositions of polymer, solvent and nonsolvent in the casting solution used to prepare different cellulose acetate (CA) membranes. 43

Table 7.2. The permeation coefficients of three model solutes through CAI, CAII and CAIII membranes. 48

Table 7.3. Morphological characteristics of CAI, CAII, CAIII membranes. 51

Table 7.4. Kinetic data for decomposition urea by native urease and urease immobilized CA membrane. 54

Table 7.5. Permeation coefficient of two solutes through urease immobilized CA membrane and regular CA membrane 56

Table 7.6. Comparison of morphological characteristics of urease immobilized and regular CA membranes. 57

Table 7.7. Input parameters used in the mathematical model shown by Equations 5.19 through 5.33. 59

Table 7.8. Mechanical properties of CAI, CAII, CAIII and urease immobilized CA membranes 72

Table 7.9. Maximum tensile stress of CA membranes. 74

CHAPTER 1

INTRODUCTION

Hemodialysis operation is an important clinical therapy to remove toxic metabolities from the blood of a patient with end-stage renal disease. Currently, approximetely one million people per year benefit from this method throughout the world. The most important element of the hemodialysis operation is the semipermeable membrane which allows the selective removal of low to medium molecular weight biological metabolities from the blood. The clinical use of hemodialysis membranes was started in 1960 and in 1992 more than 400 dialyzers produced from different polymers with different pore size and surface area were listed by the European Dialysis Transplant Association-European Renal Association (Morti et al. 2003).

An average dialysis time is usually around 3-5 hours and 3 treatments per week. High mass transfer rate through the membrane is usually desired in order to keep treatment time to a minimum. In addition, membrane must have high blood compatibility to prevent undesirable reaction of blood components at the membrane surface.

To obtain hemodialysis membranes with the desired transport and blood compatibility characteristics, an optimized surface and bulk structure is required. Structure of the membrane should also be optimized to minimize amount of protein which can adsorb on the surface. Protein adsorption not only causes a decrease in the permeability of the membrane but also induces clot formation which requires infusion of an anticoagulant into the patient. Thus, inhibition of protein adsorption is necessary to ensure steady and safe treatments of patients suffering from end-stage renal disease.

Most of the polymers used in the preparation of hemodialysis membranes are hydrophobic, thus, they are susceptible to protein adsorption. Many strategies have been developed to control adsorption on blood-contact membranes such as using asymmetric membranes, cleaning and regeneration of membranes and modification of membrane surfaces (Sun et al. 2003, Lin et al. 2004, Nie et al. 2004, He et al. 2005). Among these techniques, surface modification was frequently used as an effective approach against protein adsorption (Ye et al. 2002, Ye et al. 2003, Sun et al. 2003, Lin et al. 2004, Nie et al. 2004, He et al. 2005) Various surface modification strategies have been reported in

the literature and they have been classified into four distinct categories as introduction of negatively charged surface groups, increasing hydrophilicity, introduction of steric hindrance and biomimetic modifications. A detailed review of these methods is given in a review paper of Sun et al. (2003). To obtain excellent biocompatible and protein adsorption resistant membranes, membrane surfaces were usually coated with other polymers by physical adsorption, graft polymerization, or interpenetrating network formation.

The objective of the studies in this thesis is to prepare hemodialysis membranes with improved transport properties and reduced protein adsorption capacities. To achieve this goal, membranes were prepared from cellulose acetate by using dry phase inversion method and they were modified with an enzyme immobilization technique. Urease enzyme which can catalyze the hydrolysis of urea was directly blended into the casting solution to prepare urease immobilized cellulose acetate membranes. These membranes were characterized in terms of protein adsorption capacities, toxic solute permeation rate, stability of immobilized enzyme activity in wet and dry forms as well as structure and mechanical properties. A mathematical model was derived to determine rate of mass transfer of urea through urease immobilized CA membranes. Model predictions along with experimental studies were used to illustrate the advantage of urease immobilization on the rate of removal of urea from the blood.

This thesis consists of seven chapters except the introduction. In Chapter 2, the principal of hemodialysis operation is explained, types of commercial membranes and membrane modules and characterization tools used to test the performance of the membranes are listed. In Chapter 3, the phase inversion techniques typically used to prepare asymmetric, porous membranes are explained. In Chapter 4, a review of the strategies which were developed to control the protein fouling on blood contacting membranes is given. Chapter 5 gives a detailed derivation of transport equations used to calculate rate of mass transfer of solutes through catalytic and noncatalytic membranes. Materials and all experimental procedures are explained in Chapter 6, while results of all experimental studies and model calculations are discussed in Chapter 7. Finally, conclusions from this study and recommendations for future work are listed in Chapter 8.

CHAPTER 2

HEMODIALYSIS OPERATION

Hemodialysis is an important application for membrane separations by which low-molecular weight metabolic, toxic harmful wastes such as urea, uric acid and creatinine are removed from the blood of uremia patient. The blood of patient is allowed to flow, through a machine with a special filter that removes wastes and extra fluids. The clean blood is then returned to the body. Removing the harmful wastes and extra salt and fluids helps control blood pressure and keep the proper balance of chemicals like sodium and potassium in the blood. (WEB_1). As seen from Figure 2.1., in a typical hemodialysis system solutes and solvents are exchanged by a semipermeable membrane between blood and artificial fluid called dialysate.

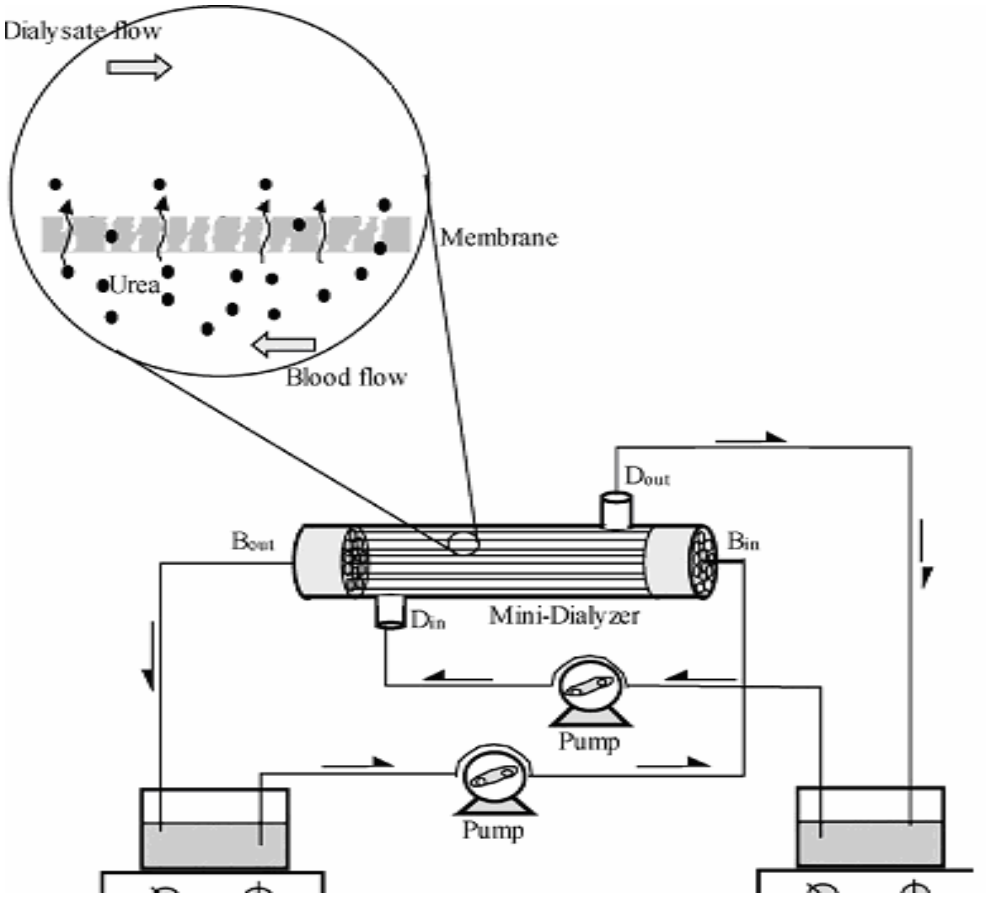

Figure 2.1. Typical Hemodialysis System.

There are 4 important equipments in a hemodialysis system (WEB_1).

i. Dialysis Machine

This machine has two main jobs as pumping blood, monitoring the flow and the blood pressure and the rate of fluid removal from the body safely (WEB_1).

ii. Dialyzer

The dialyzer is called an artificial kidney containing thousands of semipermeable membranes through which the blood is passed. The semipermeable membranes are the most important part of the dialyzer and also hemodialysis system. Dialysis solution, the cleaning fluid, is pumped around these membranes (WEB_1).

The membrane material and the design of the dialyzer determine the performance of the dialyzer. Thus the selection of the polymer material and types of dialyzers are very important issues and will be considered in this chapter in sections 2.1. and 2.2., respectively.

iii. Dialysis Solution (Dialysate)

Dialysis solution, also known as dialysate, is the fluid in the dialyzer that helps remove wastes and extra fluid from the blood. It contains chemicals that are present in the blood such as potassium, calcium, magnesium, and sodium. A specific dialysate is usually prescribed for the treatments of patients. This formula is adjusted based on blood tests and how well the patient tolerates the treatment (WEB_1).

iv. Needles

Most dialysis centers use two needles one to carry blood to the dialyzer and one to return the cleaned blood to your body. Some specialized needles are designed with two openings for two-way flow of blood, but these needles are less efficient and require longer sessions. Needles for high-flux or high-efficiency dialysis need to be a little larger than those used with regular dialyzers (WEB_1).

2.1. Types of Modules

A vital aspect of the membrane is its design and configuration. The design of the membrane determines how much blood and how sufficiently can be filtered. There are mainly 3 different types of membrane designs: hollow fiber, parallel plate and coil. Each one has disadvantages and advantages over the other, but all of them carry the same ultimate purpose.

i) The hollow fiber dialyzer is a composite of capillary, small, hollow membranes held together at each end by a clay-like potting material, and housed by a cylinder as seen in Figure 2.1. These hollow tubes are approximately the size of a strand of hair, and combined in order to provide a large surface area. Due to its large surface area, this type of dialyzer provides the best filtration performance. It also has low blood flow resistance, controlled and predictable diffusion and ultrafiltration rates, vacuum creation capacity, countercurrent flow and no membrane compliance.

ii) Parallel plate dialyzer has two or more sheets of semipermeable membranes enclosed between support structures. The components of this dialyzer are housed into a plastic container. In parallel plate dialyzers, blood flows between membrane layers while the dialysate flows over the membranes in the opposite direction. This type of module is easily fabricated, more firmly supported than the coil type and permits predictable ultrafiltration, has a lower resistance to blood flow than the coil design and capacity for vacuum due to negative pressure. However, disadvantage of this membrane is a slight compliance.

iii) The coil dialyzer is a long spiral tube of semipermeable membrane that is wound around a central core, much like a paper towel roll. The membrane layers are separated by a mesh screen material. Blood flows horizontally through the membrane while the dialysate flow vertically, creating a crosscurrent flow instead of counter current flow as in the case of other module designs. The filtration of the blood depends on positive pressure in which excess fluid (i.e. water) is pushed through the membrane. This dialyzer is also easily fabricated. However, its high blood flow resistance, unstable

support, and the blood compartments tending to have compliance expansion due to high blood pressure of compliance makes the design futile.

2.2. Types of Membranes

There are three types of membrane classified due to the material that compose it. Based on the type of the polymer used in the membrane preparation, hemodialysis membranes are classified into three categories as cellulosic, modified cellulosic and synthetic membranes (Ruthven et al. 1997).

2.2.1. Unmodified Cellulosic Membrane

The use of cellulosic membranes decreased remarkably during the past years. The reasons of this decrease are low hemocompatibility, the desire of minimization of complement activation and extending the molecular weight spectrum of solute removal (Clark and Gao 2002).

Unmodified cellulosic membranes are produced from celloboise which is naturally occurring in saccharide. Celloboise has high hydroxyl group density that causes an increase in the activation of alternative complement pathway. However cellulosic membranes had been used widely for a long time, because they have good transport properties in terms of removal of wastes from human blood. They have symmetric structure, low wall thickness and high porosity that provide them a satisfactory diffusive property for removal of small size, water soluble uremic toxins. On the other hand these membranes have quite high hydrophilic character causing fouling and ineffective adsorptive and transmembrane removal of middle or larger size uremic toxins (Clark and Gao 2002). Cuprophan, cuproammonium rayon, saponified cellulose ester are examples of unmodified cellulosic polymers (Deppisch et al. 1998, Clark and Gao 2002)

2.2.2. Modified Cellulosic Membrane

Modified cellulosic membranes has also symmetric structure and low wall thickness like unmodified cellulosic membranes but they have larger porosity which

results with higher water permeability and middle molecule size uremic toxins clearance. There are basically two types of modified cellulosic membranes depending on the molecule replacement during the modification;

- *Cellulose acetate membranes*

Approximately 75% of hydroxyl groups on the backbone of the polymer are replaced with acetate group in order to produce cellulose acetate membranes. Production of cellulose triacetate membranes involves complete hydroxyl group substitution. The complete substitution results with the decrease of the complement activation. Leukopenic response also decreases which is the white blood cell decrease from baseline usually in a range of 35-40% (Clark and Gao 2002).

- *Hemophan membranes*

In order to produce hemophan membranes only a small percentage of hydroxyl group are replaced as opposed to the preparation of cellulose acetate membranes. However, the tertiary amine replacement is more significant. The decrease in complement activation and leucopenia is approximately the same with cellulose acetate membrane (Clark and Gao 2002).

2.2.3. Synthetic Membrane

In order to solve the problems occurred with unmodified cellulosic membranes, synthetic membranes were developed. First synthetic polymeric membrane was produced in the early of 1970s. Since that time, various synthetic polymers such as polysulfone, polyamide, poly(methyl methacrylate), polyethersulfone, polyethersulfone/ polyamide have been used in the production of synthetic hemodialysis membranes (Deppisch et al.1998, Clark and Gao 2002).

Synthetic membranes have large mean pore size and thick wall structure. These properties provide high ultrafiltration rate which is necessary for hemodialysis to be achieved with relatively low transmembrane pressures (Clark and Gao 2002).

The main difference in synthetic and cellulosic membranes is chemical composition of the membrane. Synthetic membranes are made from manufactured thermoplastics, while both modified and unmodified cellulosic membranes are prepared from natural polymers (Clark and Gao 2002).

2.3. Properties of Hemodialysis Membranes

The clinical performance of a hemodialyzer is an important issue for the patient. The selection of the membrane should be carefully done assuring the safety and effectiveness during the application. Patient's quality of life should not be risked (Ruthven et al. 1997).

To ensure a successful hemodialysis operation the membrane used in the dialyzer should have some properties. First of all, high mass transfer rates through the membrane is necessary in order to shorten the treatment time. The other important demand is hemocompatibility of the membrane. Contacting of blood with a foreign surface causes activation of the blood components which results in the formation of macromolecular complexes (Deppisch et al. 1998).

In order to ensure high permeability and blood compatibility, the selected membrane should have some properties which are listed below (Deppisch et al. 1998).

a. The pore radius should have a certain size.

b. The porosity (fraction of the membrane volume which is open to the flow of solvent) of the membrane at the surface as well as in the matrix should be as high as possible to enable high transmembrane fluxes.

c. The tortuosity (i.e. the measure of the deviation of the structure from cylindrical pores normal to the surface) should be small.

d. The pore size distribution should be narrow to obtain a sharp molecular weight cut-off curve for the membrane.

e. The diffusion coefficient in the membrane should be high.

f. The smallest diameter of the pores should be on the innermost surface to prevent clogging of the solutes inside the pores.

g. The susceptibility of the membrane to protein adsorption should be limited to prevent narrowing of pores and a declining permeability during blood contact.

h. The active membrane layer (skin) should be as thin as possible, because the permeability is inversely proportional to the thickness of this layer.

The chemical composition of the membrane effects the surface properties of the membrane. In order to have desired surface properties, polymer selection is an important issue. Favorable membrane surface for hemodialysis application should not adsorb any proteins or cells but should still have a high permeability for toxic solutes in the blood.

The protein deposition on the membrane can cause instabilities of transport characteristics and a significant reduction in the in vitro solute clearance. The previous in vitro studies have shown that membranes with a balanced hydrophilicity allow a better biocompatibility because of the decrease in protein adsorption on the surface (Deppisch et al. 1998).

2.4. Characterization Tools for Hemodialysis Membranes

Five special characterization tools are used to test the performance of the hemodialysis membranes and they are listed below (Yang and Liu 2003);

- *Surface Characterization*

The surface morphology of the membrane is examined using scanning electron microscope (SEM). The hydrophilicity of the membrane can be investigated based on the contact angle of the membrane which was measured using a contact angle goniometer.

- *Porosity Determination*

The porosity of the membrane can be determined by measuring the diameter of pores from SEM photograps.

- *Tensile Strength and Elongation*

The tensile strength and elongation of the membrane can be measured using a tensile tester.

- *Adsorption of Blood Cells onto the Membrane*

Adsorption capacity of the membranes is determined by soaking the membrane into a protein solution and measuring the change in the protein concentration (Seita et al. 1997).

- *Diffusion Properties*

Diffusion coefficient of the solutes through the membrane can be determined using a simple experimental setup which consists of two compartments separated by a membrane. Donor compartment contains the solution with known solute concentration while receiver compartment initially does not contain any solute. The change in the concentration of solute in each compartment due to its transport from donor to receiver compartment is followed with time. The data is used to evaluate diffusion properties of solutes through the membrane.

CHAPTER 3

PHASE INVERSION TECHNIQUE

The invention of asymmetric membranes by Loeb and Sourirajan has made a great impact on the development of membrane science and technology. The asymmetric membranes have a very thin, relatively dense skin layer which is supported by a more open porous sublayer. The skin layer determines the permeability and imparts high selectivity while the porous sublayer provides mechanical strength. Structural characteristics of the membrane, such as fraction of the dense top layer and porous sublayer, size and shape of the pores, can be determined by the membrane preparation conditions (Altinkaya and Ozbas 2004).

Asymmetric membranes are produced by a process called phase inversion which can be achieved through four principal methods (Altinkaya and Ozbas 2004).

i) thermally-induced phase separation,
ii) vapor-induced phase separation,
iii) immersion precipitation (wet phase inversion),
iv) dry phase inversion.

In all these techniques, a homogeneous polymer solution thermodynamically separates into polymer lean and polymer rich phases. The polymer-rich phase forms the matrix of the membrane, while the polymer-lean is rich in solvents and nonsolvents.

3.1. Thermally Induced Phase Separation

The thermally induced phase-separation (TIPS) process is driven by a temperature change and it consists of five basic steps:

i) Polymer is mixed with a latent solvent referred to as diluent to form a homogeneous solution. This diluent must have high boiling point and low molecular weight so it does not cause appreciable dissolution or swelling of the polymer at room temperature.

ii) This hot polymer solution is cast onto a cold substrate in the desired shape.

iii) The cast solution is cooled to induce phase separation.

iv) The diluent that is trapped in the polymer matrix is removed during phase separation and solidification takes place to produce a microporous structure.

v) To improve the desired separation characteristics of the TIPS membrane, post-treatment processing such as stretching can be applied.

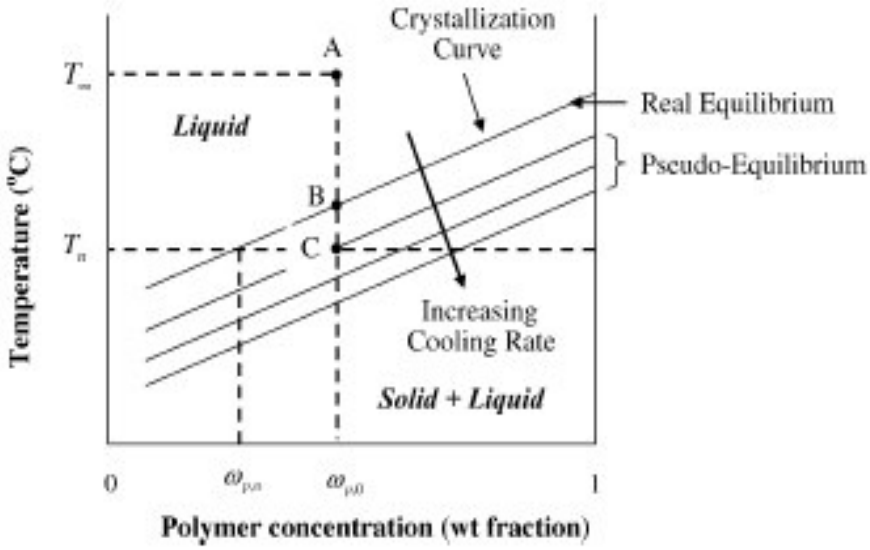

Figure 3.1. Idealized solid-liquid (S/L) TIPS phase diagram that incorporates the effect of cooling rate on crystallization to distinguish equilibrium and pseudoequlibrium conditions.

Figure 3.1. shows the solidification temperature as a function of polymer weight fraction for a polymer-diluent system. TIPS membrane formation is a nonequilibrium process, so the effect of cooling rate on the solidification temperature must be considered. The equilibrium crystallization curve is defined as the real equilibrium curve, while the crystallization curves that lie below the real equilibrium curve are called as *pseudo-equilibrium curves* since they represent nonequilibrium crystallization conditions and depend on the cooling rate.

The solution on the point A which consists of polymer/diluent mixture of composition $\omega_{p,0}$ at the temperature $T\infty$ is a homogeneous solution, however upon cooling, the solution separates into a polymer-lean phase and a pure crystalline polymer

phase. If the polymer-solution phase separates at equilibrium conditions, crystallization will be initiated on the real equilibrium curve (Point B). The solution will separate the phases at a temperature dictated by one of the pseudo-equilibrium curves (for example at Point C) as TIPS is a nonequilibrium process. The phase-separation temperature varies both in time and with position in the casting solution.

The TIPS process has particular advantages comparing to traditional phase-separation processes. TIPS can be used in a wide range of polymers to generate dense and porous films, the latter with isotropic, anisotropic or asymmetric microstructures with an overall porosity as high as 90%. Overall, the TIPS process is more flexible than wet- or dry-casting process that depend on multi-component mass transfer rather than primarily on heat transfer (Li et al. 2006).

3.2. Nonsolvent (Vapor) Induced Phase Separation

In recent years, there has been an increasing interest in nonsolvent vapor-induced phase separation (VIPS) because of its advantages in applications such as drug delivery and coating devices compared to other phase inversion techniques (Tsai et al. 2006).

During the VIPS process, phase separation is induced by penetration of nonsolvent vapour into the homogeneous polymer solution consisting of polymer and solvent(s) (Yip et al. 2006).

Relative humidity determines the driving force for a net diffusion of water vapor into the film, therefore, it has a significant influence on the VIPS phase inversion kinetics and final membrane morphology (Yip et al. 2006).

3.3. Wet Phase Inversion Method

In wet phase inversion method, a thin cast layer of the polymer solution is immersed in a nonsolvent bath. During immersion, casting solvent diffuses into the nonsolvent bath, while the nonsolvent in the bath diffuses into the solution. When the concentration of nonsolvent reaches to a critical value in the solution, then, phase seperation is initiated.

The concentration of solvent and nonsolvent in the casting solution and in the bath, respectively, the thickness and the temperature of the casting solution, as well as the temperature of the nonsolvent bath all determine the rate of mass transfer thus final structure of the membrane.

Cellulose acetate (CA) dissolved in acetone was the first polymeric material used for the preparation of membranes by the wet phase inversion process. Figure 3.2. shows the cross section morphology of cellulose acetate membrane prepared by immersing 21 % (by weight) CA solution into a water bath (Stropnik and Causer 2002).

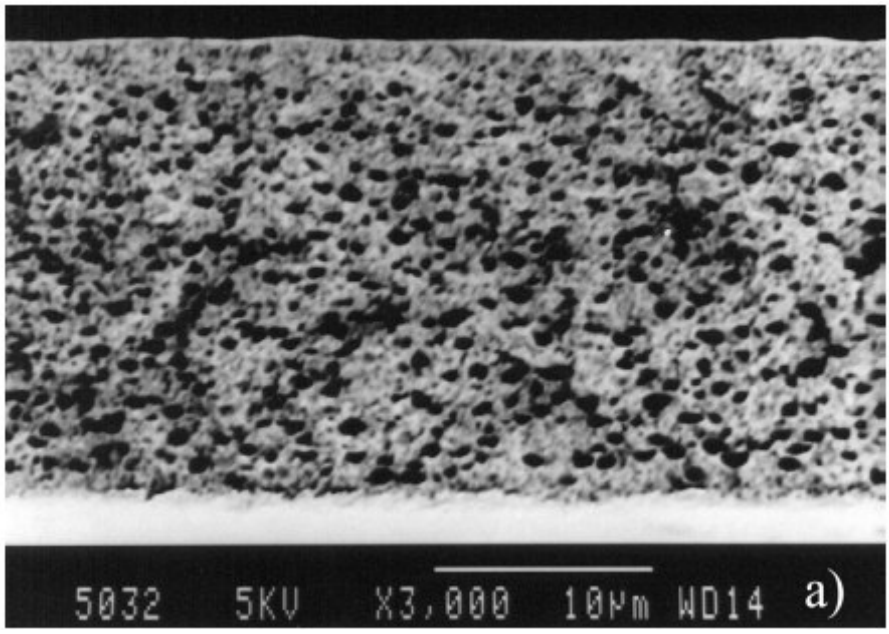

Figure 3.2. Cross section morphology of cellulose acetate membrane prepared by wet phase inversion method (Source: Stropnik and Causer 2002).

3.4. Dry Phase Inversion

In this process, the polymer dissolved in a mixture of a volatile solvent and a less volatile nonsolvent is cast on a support and expossed to an air stream. Evaporation of solvent and nonsolvent at different rates lead to a change in their concentration, thus, the polymer solution separates into polymer lean and polymer rich phases. The kinetics and thermodynamics of a phase separation process is best described in a ternary phase diagram as shown in Figure 3.3., for cellulose acetate/acetone/water system. The binodal line on the ternary phase diagram separates two phase region from one phase

region while the spinodal line seperates a metastable region from a stable two phase region. The composition paths with respect to time for the upper and lower surfaces of the evaporating solution are usually plotted on the ternary phase diagram to obtain an information about the structure of the membrane. As shown in Figure 3.3., an initially homogeneous CA solution consisting of 5% CA, 15% water and 85% acetone enters into the two phase region at 576 sec (Altinkaya et al. 2005). The difference in polymer concentration at the substrate and air facing surfaces indicate that the resulting membrane is asymmetric and porous.

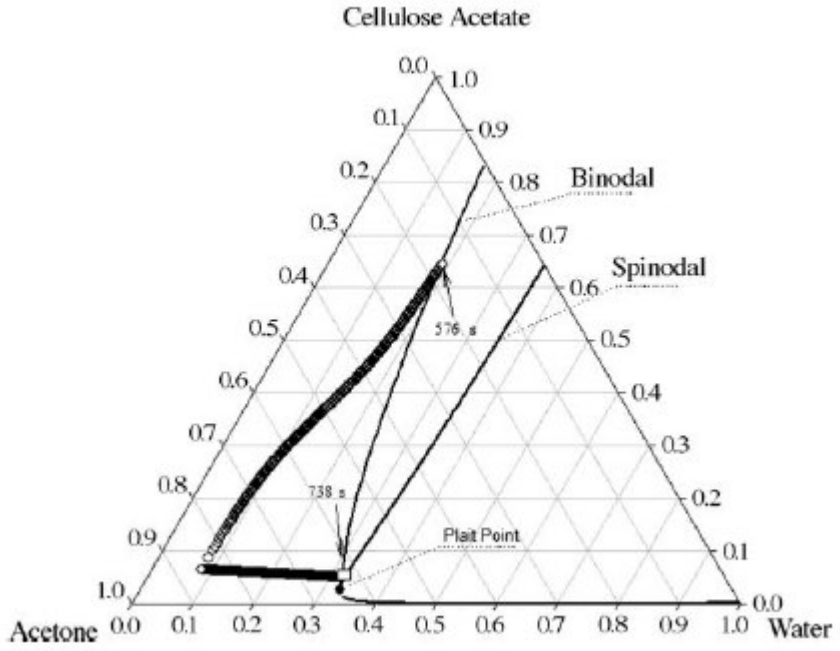

Figure 3.3. Concentration paths of water, acetone and cellulose acetate solution: (○) solution/air interface; (□): solution/substrate interface (Source: Altinkaya et al. 2005).

A recent study has indicated that the initial thickness and composition of the casting solution, the temperature and velocity of drying air as well as the relative humidity in the drying atmosphere influence the structure of the membranes prepared by the dry casting method (Altinkaya et al. 2005).

CHAPTER 4

PROTEIN FOULING ON MEMBRANES

Protein adsorption is a major problem in hemodialysis membranes, as it causes a decrease in the solute flux and change of membrane selectivity and clot formation. It is impossible to eliminate protein adsorption completely but there are some strategies to control the adsorption on the surface of blood-contact membranes.

4.1. Using Asymmetric Membrane

An asymmetric membrane includes a very thin skin layer on a highly porous and relatively thick sublayer. The size of the pores in the skin layer is very small compared to that in the sublayer. Conventional symmetric structures act as depth filters and retain most particles within their internal structure, as shown in Figure 4.1. These trapped particles plug the membrane, so the fouling occurs easily. On the other hand, asymmetric membranes are surface filters retaining all rejected materials on the surface, where most of them could be removed by shear forces applied by the feed solution moving parallel to the membrane structure as seen in Figure 4.1. Consequently, the use of asymmetric membranes, rather than symmetric ones can partially prevent the protein fouling (Sun et al. 2003).

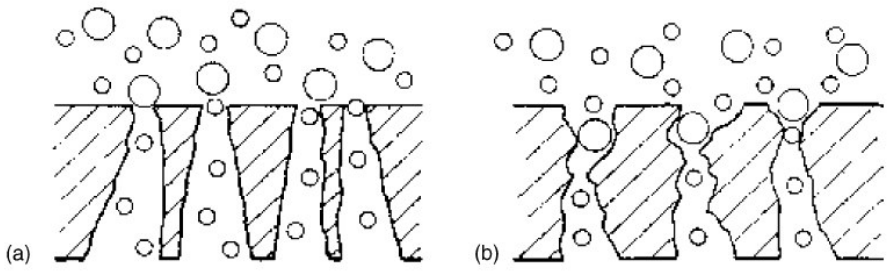

Figure 4.1. Schematic diagram of the filtration behavior of (a) an asymmetric and (b) a symmetric membrane (Source: Sun et al. 2003).

4.2. Cleaning and Regeneration of Membranes

Since mid-1970s, some scientists recommended the reuse of hemodialyzers for patients of end-stage renal disease, considering the excessive cost of clinical application of dialysis membranes. In fact, in some countries, like the United States, the recycled hemodialysis membranes are used, even though these devices were designed for a throwaway purpose. In 1994, 81% of dialysis patients in the United States were treated with recycled dialyzers. Both physical and chemical cleaning and regeneration during and after the employment can recover the efficiency of membranes (Sun et al. 2003).

4.2.1. Physical Methods

4.2.1.1. Backflushing

Backflushing is the simplest hydrodynamic method for cleaning and regeneration of membranes. In a lymphapheresis system invented by Babb (1983), as the membrane becomes plugged, a reversible pump in the system is employed to backflush the membrane for it to return to a high filtration.

4.2.1.2. Periodic Reversal of the Feed Stream

Ilias et al. (2001) and Hargrove and Ilias (2000) invented that periodical reversal of the flow direction of the feed stream could keep the system in a hydrodynamic transient state, and reduce the effect of concentration polarization and fouling. Thus, the collection of particles in a gradient near membrane surface and the particle deposition on the surface would be slowed down (Sun et al. 2003).

4.2.2. Chemical Cleaning

Chemical cleaning mainly refers to the membrane surface cleaning with various chemical reagents such as hydrogen chloride (HCl) and nitric acid (HNO_3). Dennis et al. (1986) compared four cleaning methods of hollow fiber hemodialyzers for reuse. They found that the number of times the dialyzers could be used was more than twice when a

0.3M sodium hydroxide solution was the cleaning agent, compared with the physical cleaning method. Yin et al. (2000) also found that desorption of the adsorbed human serum albumin (HSA) from membrane surface can only be achieved with NaOH .

While the practice of reusing dialyzers has become common in the United States, it is less common in West European countries and Japan. Actually, it is even prohibited in some countries, such as France. It is claimed that the relatively high mortality reported for patients receiving dialysis in the United States is associated with the reuse of the dialyzers. Cleaning and regeneration methods currently established in clinical use of dialyzers are performed off-line to permit reuse (Sun et al. 2003).

4.3. Modification of Membrane Surfaces for Antifouling

An effective method against protein adsorption is the surface modification that will change the surface characteristics of the commercial polymers either physically and/or chemically. A variety of surface modification methods have been reported, which can be roughly grouped into four distinct categories as follows (Sun et al. 2003):

- Introduction of negatively charged surface groups
- Increasing hydrophilicity
- Introduction of steric hindrance
- Biomimetic modifications

The methods mentioned above and their combinations are utilized for the modification of the membrane surface. A basic principle of modifying the membrane surface is to obtain desired bulk properties, including pore sizes and pore size distribution.

4.3.1. Introduction of Negatively Charged Surface Groups

It is usually claimed that the introduction of negative charges on the membrane surface should decrease protein fouling by increasing the electrostatic repulsion between the membrane surface and mostly negatively charged proteins and cells in blood. Chen et al. (1992) treated a ultrafiltration membrane with anionic surfactants to

reduce the adsorption of proteins. They found that small anionic surfactant reduce protein adsorption by altering electrostatic interactions between proteins and membrane surface. When nonionic surfactants or when polyethylene oxide (PEO) segments were added to the backbone of the membrane, the anionic surfactants showed significant flux improvement and fouling resistance. Higuchi et al. (1990) and Nakagawa (1990) chemically modified both the inner and the outer surfaces of polysulfone (PSF) hollow fibers with propane sultone and some Friedel-Crafts catalysts. Their results indicated that the modified fibers having hydrophilic surfaces showed better antifouling property compared with the unmodified ones. Lin et al. (2004) modified the polyacrylonitrile (PAN) by covalently immobilizing chitosan (CS)/heparin (HEP) onto the surface. The influence of surface modification on the protein adsorption and platelet adhesion, metabolites permeation and anticoagulation activity of resulting membrane was investigated. The immobilization of polyelectrolyte complex PEC caused the water contact angle to reduce that showed an increase in the hydrophilicity. Protein adsorption, platelet adhesion, and thrombus formation were all reduced by the immobilization of HEP as seen in Table 4.1., Figure 4.2. and Figure 4.3., respectively (Lin et al. 2004).

Table 4.1. Plasma protein adsorption onto the PAN membrane (Source: Lin et al. 2004).

Membrane Type	**HAS* adsorption ($\mu g/cm^2$)**	**HPF** adsorption ($\mu g/cm^2$)**	**HAS/HPF ratio (%)**
PAN	**279.7±14.9**	**564.3±16.1**	**49.6**
PAN-A	**261.7±12.5**	**501.3±15.2**	**52.2**
PAN-C	**288.3±13.9**	**615.3±14.3**	**46.8**
PAN-H	**145.4±11.9**	**211.3±12.7**	**68.8**
PAN-C-H	**108.3±12.5**	**147.9±15.6**	**73.2**

* Human Serum Albumin

** Human Plasma Fibrinogen

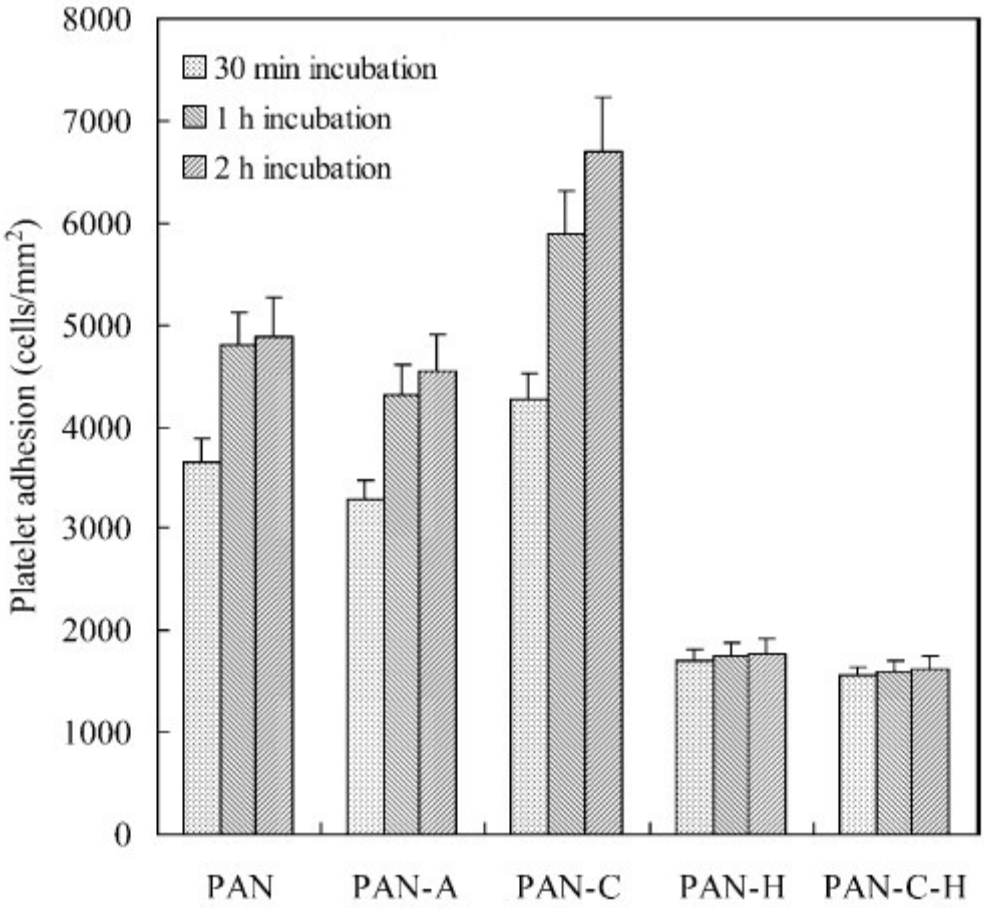

Figure 4.2. Comparison of platelet adhesion on membranes after 30 min, 1 and 2 h incubation. PAN-A represents Polyacrylonitrile + acrylic acid; PAN-C represents Polyacrylonitrile + chitosan; PAN-H represents Polyacrylonitrile + heparin; PAN-C-H represents Polyacrylonitrile + chitosan + heparin (Source: Lin et al. 2004).

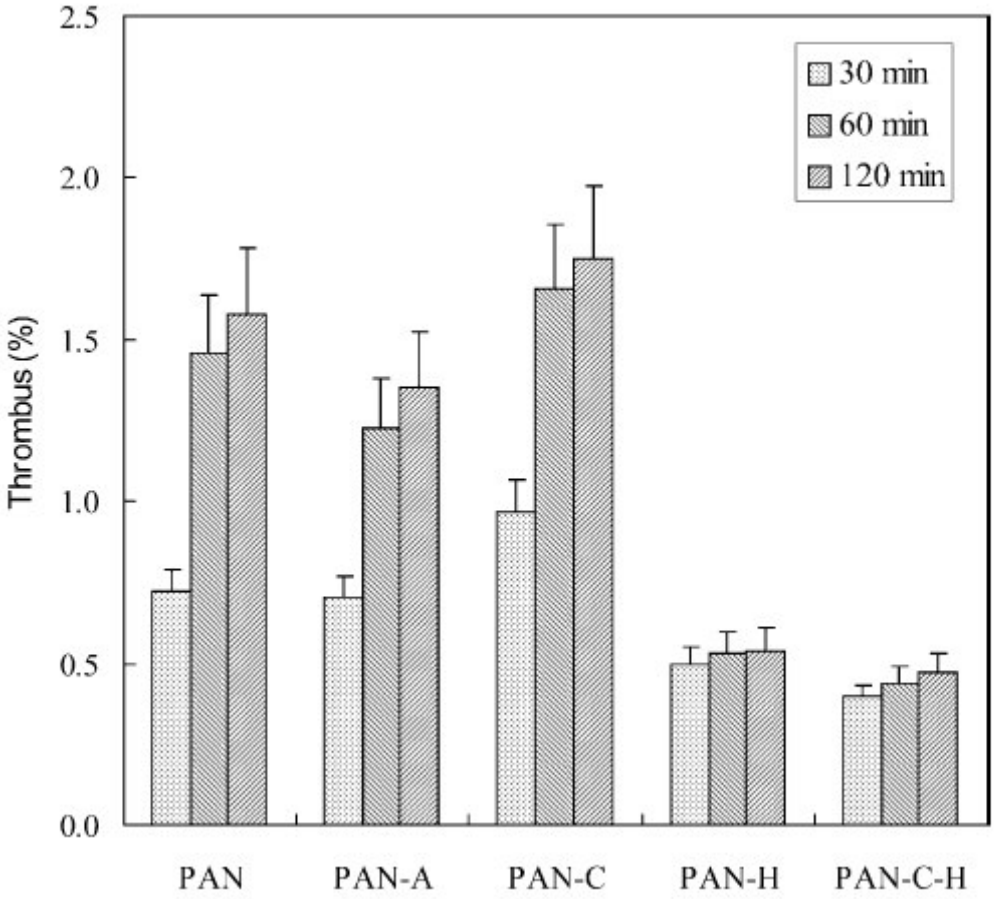

Figure 4.3. Comparison of thrombus formation on membranes after 30 min, 1 h and 2 h incubation (Source: Lin et al. 2004).

4.3.2. Increasing Hydrophilicity

It is hypothesized that hydrogen bond formed between the hydrophilic surface and water may decrease protein adsorption since proteins must first displace water molecules on the surface which requires significant amount of energy, thus, it does not occur instantaneously. Various studies exist in the literature which concentrated on the strategies to increase the hydrophilic character of the surfaces. For example, Woffinfin and Hoenich (1988) decreased the degree of complement activation and leucopenia in blood associated with the use of cellulosic membranes by adjusting the ratio of hydrophobic segments.

Nie et al. (2004) improved the anti-fouling properties and blood compatibility of poly(acrylonitrile-co-maleic acid) (PANCMA) membranes by the immobilization of

poly(ethylene glycol)s (PEG) on membrane surface. They found that the reactive carboxyl groups on PANCMA membrane surface could be conveniently conserved into anhydride groups then esterified with PEG. The hydrophilicity and blood compatibilityof the acrylonitrile-based copolymer membranes were improved with the immobilization of PEG. Compared with the original PANCMA membrane, the membrane immobilized with PEG showed a three-fold increase in a bovine serum albumin (BSA) solution flux, a 40.4% reduction in total fouling, and a 57.9% decrease in BSA adsorption (Nie et al. 2004).

Coating, blending and grafting techniques were commonly used to introduce an hydrophilic character into traditional hydrophobic membranes. These techniques are discussed below.

4.3.2.1. Physical Coating

Physical coating is one of the oldest methods used for modifying the surface properties. In this technique, a hydrophobic membrane is coated with a hydrophilic polymer. For example, in Brink's et al. (1993) study polysulfone (PSF) UF and microfiltration (MF) membranes were coated with two water-soluble polymers. Protein adsorption at the pore walls of the UF membranes was prevented, however, coating of the surface could not stop the plugging of the pores by the proteins. Ye et al. (2005) modified celulose acetate membrane with the water-soluble amphiphilic 2-methacryloyloxyethyl phosphorylcholine (MPC) and its copolymer butyl methacrylate (BMA). PMB80 (MPC: BMA=80:20 mol %) was coated on the CA hollow fiber membrane surface during the phase inversion of the dope solution by using a PMB 80 solution as inner coagulant. The CA/PMB80 coated hollow fiber membrane showed low membrane fouling property compared with the unmodified CA hollow fiber membrane, due to the low protein adsorption property of the PMB80.

Modification of the surfaces by coating with hydrophilic polymers has generally been found not a successful approach due to desorption of the coating easily in a short period of time after its initial use (Sun et al. 2003).

4.3.2.2. Blending

Blending is another simple modification technique used to increase hydrophilic character of the hydrophobic membranes. In this technique, a hydrophilic polymer is directly added into the casting solution and it is distributed evenly both on the membrane surface and within the matrix. Many studies exist in the literature which utilizes this approach for modifying membrane surfaces (Sun et al. 2003).

Ward and co-workers (1998) modified the hydrophobic PSF membrane by blending it with polyvinyl pyrrolidone (PVP). They found that surface hydrophilicity increased with the increased PVP content in the solution. T. Hasegawa et al. (2001) prepared a polymer blend composed of polysulfone and 2-methacryloyloxyethyl phosphorylcholine (MPC) polymer (PSf/MPC polymer) and obtained asymmetric porous membrane by the dry/wet membrane processing method. It was found that amount of protein adsorbed on the PSf membrane from plasma was reduced by the addition of the MPC polymer and platelet adhesion was also effectively suppressed on the PSf/MPC polymer membrane. In addition, the reduction in permeabilities due to protein fouling was found to be smaller with blend membranes. As an illustration, Figure 4.4. shows the permeation coefficient of cytochrome C through PSF and PSF/MPC blend membranes before and after contact with protein solution.

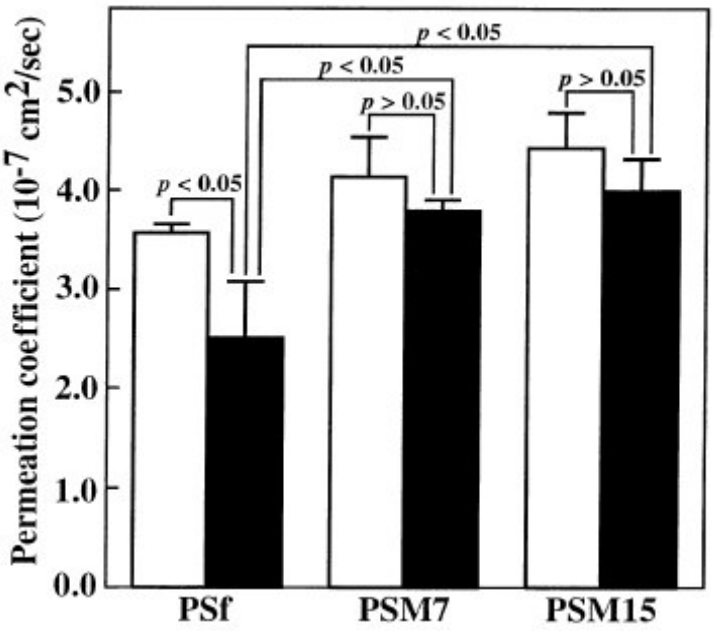

Figure 4.4. Permeation coefficient for cytochrome C through the asymmetric porous membranes before (white bar) and after (black bar) contact with protein solution. PSM7 represents PSf+7%wt 2-methacryloyloxyethyl phosphorylcholine (MPC) polymer, PSM15 represents PSf+15%wt MPC polymer (Source: Hasegawa et al. 2001).

S. H. Ye et al. (2002) improved the blood compatibility of cellulose acetate (CA) by blending a CA membrane with PMB30 (amphiphilic 2-methacryloyloxyethyl phosphorylcholine (MPC) and its copolymer butyl methacrylate (BMA)). Both the original CA and the blend membrane had an asymmetric and porous structure. The mechanical properties and solute permeability of the CA/PMB blended membrane were controlled by preparation conditions. By blending with PMB, the membrane showed good permeabilities for water and solutes in comparison with the original CA membrane. Figure 4.5. shows the adsorption pattern of proteins on the surfaces of the CA membrane detected by gold-colloid-labeled immunoassay for each protein after contact with human plasma for 90 min. Small white particles correspond to the specific protein adsorbed in the membrane. The result clearly indicates that protein adsorption capacity of CA/PMB30 blend membrane is lower than that of CA membrane.

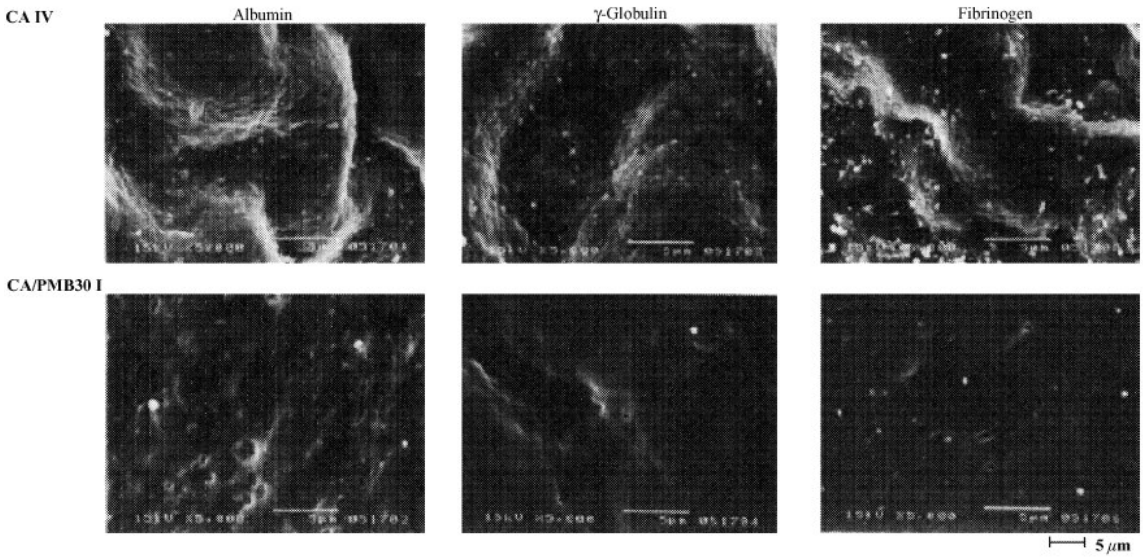

Figure 4.5. Adsorption pattern of plasma proteins on CA and CA/PMB30 blend membrane surfaces after contact with human plasma for 90 min (Source: Ye et al. 2002).

S. H. Ye et al. (2003) blended cellulose acetate (CA) membrane with poly(2-methacryloyloxyethyl-phosphorylcholine (MPC)-co-n-butyl methacrylate (BMA)) (PMB30) to improve the anti-fouling property of CA membranes. Figure 4.6. shows that protein adsorption capacity of CA membrane is lower than that of hydrophobic PSF membrane. However, it is possible to further reduce the amount of protein adsorbed on the CA membrane by blending CA with PMB30 during the casting process.

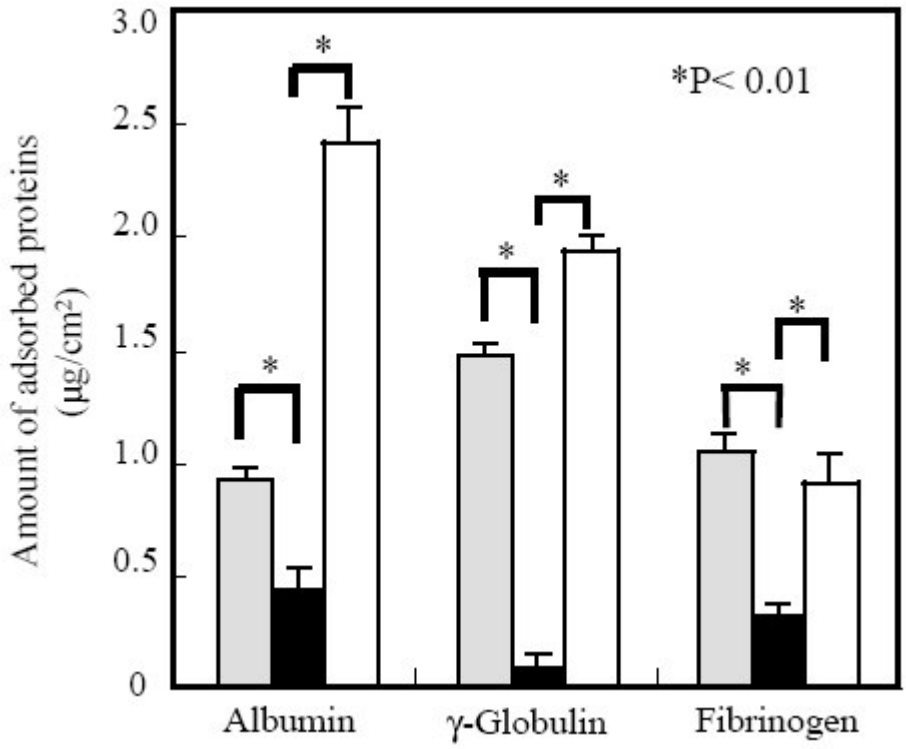

Figure 4.6. Amount of proteins adsorbed on CA (hatched bar) and CA/ PMB30 (black bar) and polysulfone (white bar) membranes (Source: Ye et al. 2003).

4.3.2.3. Chemical Modification

Chemical modification on the surface of hydrophobic membranes introduces hydrophilic segments only on the surface, thus resulting membrane presents the advantages of both hydrophilic and hydrophobic membranes. Because only the membrane surface is modified, the original characteristics of mechanical strength and thermal stability are kept. In addition, since the introduced hydrophilic segments are chemically bonded on the surface, they are more stable and do not easily elute compared with blend membranes.

Wang et al. (2000) introduced peroxide onto the membrane surface by ozone treatment followed by graft polymerization with hydroxyethyl methacrylate (HEMA) in the hydrophilic modification of polypropylene (PP) flat sheet MF membranes. The HEMA grafting made the surface of the PP membrane hydrophilic and more resistant to BSA proteins.

4.3.2.4. Photochemical Modification

Photo-induced grafting method is favored by some researchers. Ulbricht et al. (1996) modified a PAN UF flat sheet membrane with various poly(ethylene glycol) methacrylates by UV irradiation-initiated graft polymerization, using benzophenone as initiator. The results of UF experiments with γ-globulins, protein/polymer surface interactions were diminished.

4.3.2.5. Irradiation

Polyethersulfone (PES) UF hollow fiber membranes were modified by grafting PEG on the internal surface using γ-ray irradiation method by Mok et al.(1994) The fouling of hollow fibers decreased after modification.

4.3.2.6. Plasma Polymerization

Plasma polymerization of gases present in a low temperature plasma is also a "clean" technique suitable for biomedical material processing (Sun et al. 2003). Early in 1991, Clarotti et al. studied the possibilities of this technique to prepare membranes with the required bio-and hemocompatibility to be implanted in an organism. They have deposited a mixture of ethylene oxide and perfluorohexone on PSF membranes to optimize surface properties of PSF membranes without affecting their filtering properties.

4.3.3. Introduction of Steric Hindrance

In order to obtain attractive non-fouling membranes. It was suggested that low grafting degrees of hydrophilic polymer and intermediate wettabilities are sufficient. However, as the density of hydrophilic polymers grafting onto the hydrophobic surface is high enough, their chains are forced to stretch away from the surface. A hydrophilic "brush" on the surface are formed by the grafting polymer. In this so-called "brush regime", a high degree of protein rejection is generally observed for a variety of proteins. Hydrophilic brushes resist protein adsorption and cell adhesion. A lot of

researchers studied the mechanism of the protein-resistance character of polyethylene oxide (PEO) brushes, and found that the protein-resistance character of PEO was dependent on the chain length and surface density of PEO. Usually, polymer brushes on solid surfaces can be prepared by (1) irreversible adsorption of diblock or triblock copolymer chains on the surface or (2) chemical grafting (Sun et al. 2003).

4.3.3.1. Irreversible Adsorption

Over the last decade, in order to reduce the protein adsorption, various researchers have investigated the potential use of adsorbed amphiphilic diblock and triblock copolymers on solid substrates (Sun et al. 2003).

Hester and Mayes (2002) prepared immersion precipitated membranes with increased adsorption resistance from blends of polyvinylidene difluoride (PVDF) and a free-radically synthesized amphiphilic comb polymer having a methacrylate backbone and PEO side chains. X-ray photoelectron spectroscopy (XPS) analysis indicated substantial surface segregation of comb polymer during membrane coagulation, resulting in hydrophilic surfaces with excellent stability.

4.3.3.2. Chemical Grafting

Preparation of polymer brushes can also be achieved through chemical binding of performed polymer chains. The resulting polymer phase is highly stable in contrast to coated polymer phases, since polymer chains are covalently bonded to the surface. Two techniques can be employed in chemical grafting:

(a) “grafting from”, where polymer layers are formed by in situ polymerization initiated by the immobilized initiators on the surface

(b) “grafting to”, where the end-functionalized polymers are synthesized and reacted with appropriate groups immobilized on the substrate (Sun et al. 2003).

Grafting technique was applied to graft PVP on zirconia surface to study its behavior of reducing lysozyme adsorption by Rovia-Bru et al. Firstly, they modified the –OH groups presented on the ceramic particle surface by silylation with vinyltrimethoxysilane in order to generate vinyl surface sites. Then, the silylated particles were dispersed in an aqueous vinylpyrrolidone solution, and heated to the

desired reaction temperature to start the PVP graft polymerization. With this kind of technique, diffusion limitations and steric hindrance effects are minimized owing to the much smaller size of the monomeric units diffused to react with surface chains or active surface sites. Therefore, it is possible to achieve a higher degree of surface coverage than via the "grafting to" technique, though it is difficult to get monodispersed brushes (Sun et al. 2003).

4.3.4. Biomimetic Modifications

Biomimetic modifications refer to mimic a biologic surface in nature and it is a potential technique for reducing protein adsorption for synthetic polymeric membranes. The red blood cell plasma membrane naturally resists protein fouling and this is attributed to the unique phospholipid bilayer structure of the membrane (Hayward et al. 1984). Since the phospholipid constituting membranes have high mobility and don't bond covalently, they are physically and chemically unstable. Phospholipid molecules with polymerizable group are usually synthesized in order to improve its mechanical strength (Sun et al. 2003). Ishihara et al. (1990) blended MPC polymer with conventional polymeric materials used in the biomedical field. While increasing protein adsorption resistance, the mechanical strength of this blend polymer membrane did not change.

Most of these biological modifications are hydrophilic in nature, and they may also introduce negatively charged side groups onto the membrane surface (Sun et al. 2003).

CHAPTER 5

TRANSPORT OF SOLUTES THROUGH HEMODIALYSIS MEMBRANES

5.1. Transport of Solutes Through Noncatalytic Membranes

In this study, the transport of solutes through the hemodialysis membranes was studied using a diffusion cell as shown in Figure 5.1., below.

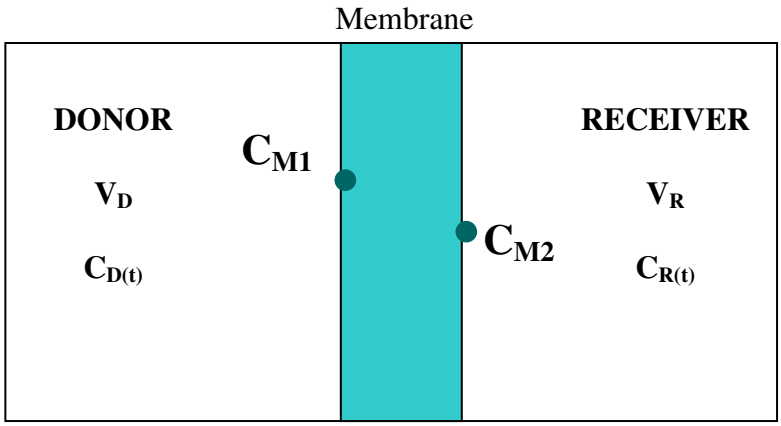

Figure 5.1. Schematic diagram of a diffusion cell.

The cell consists of two compartments and the membrane with a thickness of L and area of A is placed between the compartments. The solution in each compartment is well mixed to eliminate concentration gradients, thus, concentration of solute in each compartment only changes with time. It is assumed that mass transfer through the membrane is one dimensional and steady-state condition is reached in a short period of time in the membrane since the volume of the membrane is very small compared to the volume of the solution in each compartment. Furthermore, it is assumed that mass transfer through the membrane is dominantly by diffusion.

Under these assumptions, the overall mass balances on the donor and receiver compartments are written as follows;

$$\frac{dm_D}{dt} = V_D \frac{dC_D}{dt} = (-JA)_{x=0} \tag{5.1}$$

$$\frac{dm_R}{dt} = V_R \frac{dC_R}{dt} = (+JA)_{x=L} \tag{5.2}$$

where V_D and V_R are the liquid volumes in the donor and receiver compartments, respectively, t is time, C_D and C_R are the concentration of solute in the donor and receiver compartments, respectively and J is the diffusive flux, defined as follows using Fick's law:

$$J = -D_{AB} \frac{dC_A}{dx} \tag{5.3}$$

where D_{AB} is the diffusivity and C_A is the concentration of the solute across the membrane. Under steady state conditions with no chemical reaction in the membrane, the rate of transfer of solute through the membrane becomes constant, i.e.,

$$JA_{x=0} = (JA)_{x=L} \tag{5.4}$$

$$JA_{x=0} - (JA)_{x=L} = 0 \tag{5.5}$$

If Equation 5.3 is integrated from x=0 to x=L, then, the rate of mass transfer of solute through the membrane is calculated as follows:

$$JA = \frac{D_{AB}(C_{M1} - C_{M2})A}{L} \tag{5.6}$$

where C_{M1} and C_{M2} are the concentrations of permeating solute at the boundaries of the membrane. If it is assumed that linear equilibrium relationship exists between the concentration of the solute in the solution and at the membrane surface, then C_{M1} and C_{M2} can be expressed as follows;

$$C_{M1} = KC_D \qquad C_{M2} = KC_R \tag{5.7}$$

where K is the partition coefficient of the solute between the membrane and the adjacent phase. If equation 5.7 is inserted into equation 5.6, then

$$JA = P_{eff} A(C_D - C_R) \tag{5.8}$$

where, P_{eff} is defined as follows:

$$P_{eff} = \frac{D_{AB} K}{L} \tag{5.9}$$

If Equation 5.8 is inserted into the Equations 5.1 and 5.2,

$$V_D \frac{dC_D}{dt} = -P_{eff} A(C_D - C_R) \tag{5.10}$$

$$V_R \frac{dC_R}{dt} = -P_{eff} A(C_D - C_R) \tag{5.11}$$

and if Equation 5.10 is substracted from Equation 5.11, then

$$\frac{d}{dt}(C_D - C_R) = \beta(C_D - C_R) \tag{5.12}$$

where ß is a geometric constant, defined as follows:

$$\beta = [\ \frac{1}{V_D} + \frac{1}{V_R}\ ] P_{eff} A \tag{5.13}$$

Finally, Equation 5.12 is rearranged and integrated from t=0 to t=t with the initial conditions

$$C_{D_{t=0}} = C_{Di} \qquad\qquad C_{R_{t=0}} = C_{Ri} \tag{5.14}$$

to obtain following expression.

$$\ln \frac{C_{D_i i} - C_{Ri}}{C_D - C_R} = \beta t \tag{5.15}$$

If it is assumed that there is no accumulation in the membrane,

$$m_{tot} = C_{Di}V_D + C_{Ri}V_R = C_D V_D + C_R V_R \tag{5.16}$$

where m_{tot} is the total amount of solutes in both receiver and donor compartments. Combining Equations 5.15 and 5.16, time dependence of the concentration of the solutes in the donor and the receiver can be obtained as follows:

$$C_D = \frac{C_{Di}}{1+\frac{V_R}{V_D}} + \frac{1}{1+\frac{V_D}{V_R}}\left[C_{Ri} + \left(C_{Di} - C_{Ri}\right)\exp\left(-P_{eff}\beta t\right)\right] \tag{5.17}$$

$$C_R = \frac{C_{R_0}}{1+\frac{V_D}{V_R}} + \frac{1}{1+\frac{V_R}{V_D}}\left[C_{Di} - \left(C_{Di} - C_{Ri}\right)\exp\left(-P_{eff}\beta t\right)\right] \tag{5.18}$$

5.2. Transport of Solutes Through Catalytic Membrane

The model developed in this section considers the transport of a solute through a membrane in which the solute is decomposed by immobilized enzyme. The enzymatic decomposition of solutes is best described by Michaelis-Menten equation given as follows:

$$V = \frac{V_{max} C_A}{K_m + C_A} \tag{5.19}$$

where V is the rate of decomposition of solute, K_m and V_{max} values are Michaelis-Menten constants that are used to determine the enzyme kinetics and C_A is the concentration of solute at any position in the membrane. If it is assumed that $K_m \gg C_A$, then the rate expression becomes linear as follows:

$$V = \frac{V_{max}}{K_m} C_A \tag{5.20}$$

The species continuity equation for the solute through the catalytic membrane is given by Equation 5.21.

$$D_{AB}\frac{d^2C_A}{dx^2} - \frac{V_{\max}}{K_m}C_A = 0 \tag{5.21}$$

Equation 5.21 is a linear, homogeneous, second-order differential equation with constant coefficients. Its general solution is given by Equation 5.22.

$$C_A(x) = C_1 e^{mx} + C_2 e^{-mx} \tag{5.22}$$

where

$$m = \sqrt{\frac{V_{\max}}{K_m D_{AB}}} \tag{5.23}$$

and C_1 and C_2 are constants which are evaluated from the following boundary conditions

$$C_A(x=0) = C_{M1} \qquad C_A(x=L) = C_{M2} \tag{5.24}$$

$$C_1 = \frac{C_{M2} - C_{M1}e^{-mL}}{e^{mL} - e^{-mL}} \tag{5.25}$$

$$C_2 = C_{M1} - C_1 \tag{5.26}$$

The concentration profile of the solute through the membrane is then given by the following expression:

$$C_A(x) = \left(\frac{C_{M2} - C_{M1}e^{-mL}}{e^{mL} - e^{-mL}}\right)e^{mx} - \left(\frac{C_{M2} - C_{M1}e^{mL}}{e^{mL} - e^{-mL}}\right)e^{-mx} \tag{5.27}$$

The fluxes of the solute at the boundaries of the membrane are calculated using Fick's low (Equation 5.3) and the concentration profile of the solute through the membrane (Equation 5.27).

$$(J)_{x=0} = -D_{AB}\left(\frac{dC_A}{dx}\right)_{x=0} \tag{5.28}$$

$$(J)_{x=L} = -D_{AB}\left(\frac{dC_A}{dx}\right)_{x=L} \tag{5.29}$$

The results are given in Equations 5.30 and 5.31, as follows:

$$(J)_{x=0} = D_{AB}\left\{\frac{C_{M1}e^{mL} - C_{M2}}{e^{mL} - e^{-mL}} + \frac{C_{M1}e^{-mL} - C_{M2}}{e^{mL} - e^{-mL}}\right\}m \tag{5.30}$$

$$(J)_{x=L} = D_{AB}\left\{\frac{C_{M1}e^{mL} - C_{M2}}{e^{mL} - e^{-mL}}e^{-mL} + \frac{C_{M1}e^{-mL} - C_{M2}}{e^{mL} - e^{-mL}}e^{mL}\right\}m \tag{5.31}$$

Finally Equations 5.30 and 5.31 are inserted into Equations 5.1 and 5.2 to obtain expressions for the time rate change of solute concentration in the donor and receiver compartments.

$$\frac{dC_D}{dt} = -\frac{A}{V_D}D_{AB}\left\{\frac{C_{M1}e^{mL} - C_{M2}}{e^{mL} - e^{-mL}} + \frac{C_{M1}e^{-mL} - C_{M2}}{e^{mL} - e^{-mL}}\right\}m \tag{5.32}$$

$$\frac{dC_R}{dt} = \frac{A}{V_R}D_{AB}\left\{\frac{C_{M1}e^{mL} - C_{M2}}{e^{mL} - e^{-mL}}e^{-mL} + \frac{C_{M1}e^{-mL} - C_{M2}}{e^{mL} - e^{-mL}}e^{mL}\right\}m \tag{5.33}$$

Equations 5.32 and 5.33 can be integrated numerically to obtain concentration of solute in the donor and receiver compartments.

CHAPTER 6

EXPERIMENTAL STUDIES

Experimental studies in this thesis can be grouped into five categories as membrane preparation, protein adsorption, permeation, immobilized enzyme activity determination and characterization studies.

6.1. Materials

Membranes were prepared from ternary solutions consisting of cellulose acetate, acetone and water. Cellulose acetate (CA) with a molecular weight of 50000g/mol and an acetyl content of 39.8 % was purchased from Sigma. Aceton with a purity of »99%, bovine serum albumin (MW 65000), urea (MW 60.06), creatinine (MW 113.12), uric acid (MW 168.11) were also purchased from Sigma.

Urease (E.C.3.5.1.5) from jack beans and H_2NaPO_4, were purchased from Fluka. Na_2HPO_4, used for buffer solutions was purchased from Riedel. Phenol, sodium-nitroprusside dihydrate, sodium-hypochlorite were obtained from Merck, acedic acid was obtained from Aldrich and NaOH was purchased from Sigma. Water used in the experiments was distilled ion-exchanged water.

6.2. Preparation of Membranes

The cellulose acetate was dissolved in acetone and water was added and the solution was stirred for 6 hours until it becames homogeneous. Then, stirring was stopped and the solution was waited for 18 hours in order to let collapse of bubbles in it. The solution was cast onto 10cm x 24cm glass substrate with the aid an automatic film applicator (Sheen Instrument Ltd., model number:1133N) with 100 mm/sec. The initial thickness of the cast film was adjusted by a four sided applicator with the gap size of 300 µm. Immediately after casting, the support was transferred into an environmental chamber (Angelantoni Industrie, Italy, Challenge Series, model number:CH250) in which the solution was dried for 2 h under 25ºC temperature and 40% relative humidity.

Membranes were allowed to dry further for a period of 24 h in a vacuum oven maintained at 100ºC. They were then kept in a desiccator until their use.

To prepare urease immobilized membranes 0.5 g of cellulose acetate was dissolved in 10.2 ml of acetone and 50 mg of urease dissolved in 1.45 ml of water. The polymer and enzyme solution were mixed and stirred for 30 minutes. Then, the solution was cast on a glass substrate with a knife of 300 µm gap and dried in the environmental chamber for 2 hours under 25ºC temperature and 40% relative humidity. Membranes used for determining uric acid and creatinine permeation rates were immersed in a phosphate buffer solution at 4ºC for a period of 24 hours in order to remove soluble and weakly bonded enzyme. On the other hand, membranes used for the removal of urea were not kept in phosphate buffer solution in order to not loose urease activity. All urease immobilized membranes were kept in the refrigerator until they are used for the next experiment.

6.3. Protein Adsorption Experiments

Bovine serum albumin (BSA) solution was prepared in 0.05 M, pH 7.4 phosphate buffer with a concentration of 0.4 mg/ml. Membranes were immersed in BSA solution and maintained at 37ºC for at least 24 hours. During incubation period, 20 µL samples were taken at certain time intervals in order to determine BSA concentration in the solution. BSA content in the solution was determined using a rapid and sensitive Bradford method which utilizes the principle of protein-dye binding (Bradford 1976). During the application of the method, 20 µl of BSA containing solution was mixed with 1 ml of dye reagent prepared from Coomassie Brilliant Blue G-250 and 50 µl of NaOH. The resulting solution was incubated at room temperature for 15 minutes and the absorbance at 595 nm was measured by a spectrophotometer (Perkin Elmer Model No: Lambda 45).

6.4. Determination of immobilized urease activity

Enzyme activity was calculated by measuring the amount of ammonia produced enzymatically, using urea as a substrate. The reaction is shown below:

$$H_2NCONH_2 + 2H_2O \xrightarrow{\text{urease}} 2NH_3 + CO_2$$

The amount of ammonia produced was determined spectrophotometrically by using reaction of phenol with hypochlorite by the method reported by Weatherburn (1967). Two reagents are used in this method and they were prepared as follows:

Reagent A: 5 g of phenol with 25 mg of sodium-nitroprusside were dissolved in distilled water and made up to 500 ml.

Reagent B: 2.5 g of sodium hydroxide was dissolved in distilled water and made up to 500 ml.

For determination of immobilized urease activity, a 7 cm² membrane was immersed into 25 ml of 100 µM urea solution that was prepared in 0.05 M pH 7.4 phosphate buffer solution. Before immersing the membranes, urea solution was incubated for 30 minutes at 37 ºC. The membrane was kept in the solution for a period of 90 minutes and during this period, the solution was maintained at 37 ºC and continuously stirred with a speed of 200 rpm.

After reaction started, 1 ml samples were taken at 45 and 90 minutes and each 20µl volume from this sample was pipetted into two tubes. In order stop the reaction 10% acetic acid solution was added into each test tube. Then, 5 ml of reagent A was added, stirred sufficiently and 5 ml reagent B was mixed throughly. The test tubes were incubated at 37ºC for a period of 20 minutes to observe color change which corresponds to ammonia evolution. The absorbance of the solution was measured at 625 nm against a 20µl phosphate buffer solution.

The activity of urease was calculated from the production rate of NH_3 per minute.

$$Activity = \left(\frac{\text{Number of moles of } NH_3 \text{ produced in 45 min}}{(45 \text{ min}) \times (\text{cm}^2 \text{ of the membrane})} \right) \tag{6.1}$$

To determine amount of ammonia produced enzymatically, calibration curve was formed by dissolving different amounts of ammonium sulfate ($(NH_4)_2SO_4$) in water and measuring the ammonium concentrations of resulting solutions by the Weatherburn

method. $(NH_4)_2SO_4$ gives a reaction with the reagents to produce ammonium ion and sulfate ion as shown below:

$$(NH_4)_2SO_4 \longrightarrow 2NH_4^{+} + SO_4^{2-}$$

$$NH4^{+} + OH^{-} \longrightarrow NH_3 + H_2O$$

6.4.1. Determination of Immobilized Urease Stability in Buffer

To determine stability of immobilized urease with time, four pieces of membranes were immersed into 25 ml of 0.05 M phosphate buffer solution at pH 7.4, 37 ºC. The solution was stirred throughly and the membrane samples were removed from the solution at 30, 60, 120 and 180 minutes successively to determine the activity of the immobilized urease.

6.4.2. Determination of Immobilized Urease Stability in Dry Membrane

To determine the stability of immobilized urease enzyme in dry storage, membranes were stored in dry form at 4°C for 8 weeks and the activity of enzyme were measured at different times.

6.5. Permeation Experiments

Permeation experiments were carried out in a side by side diffusion cell (Permegear Membrane Transport Systems) as shown in Figure 6.1. The membrane was placed in the middle of the two parts of the cell. The left-side (Donor) chamber was filled with 5 ml phosphate buffer (pH 7.4) containing desired amount of solute, while the right-side (Receiver) chamber was only filled with phosphate buffer (pH 7.4).

The solution in each chamber was stirred sufficiently to eliminate concentration gradient and temperature was maintained constant at 37ºC by circulating water through the jacket which surrounds the chambers. Samples were removed from each chamber at

certain time intervals and concentration of each solute was determined by a UV-Spectrophotometer.

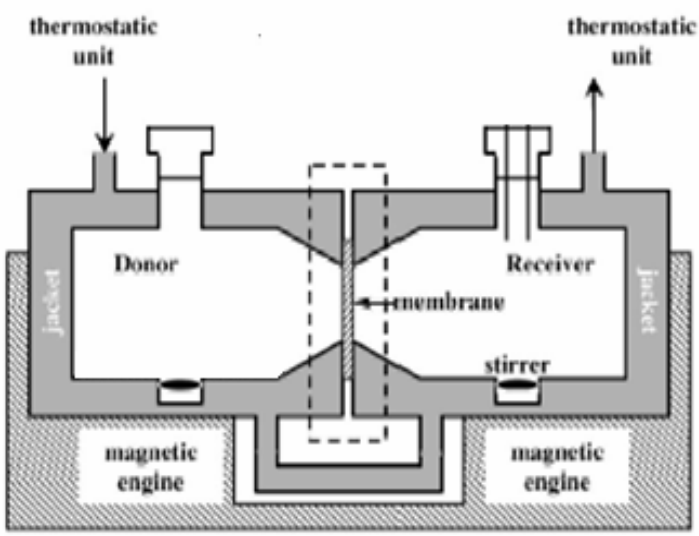

Figure 6.1. Experimental set-up used for permeation experiments.

The concentration of uric acid was determined by directly measuring its absorbance at 285 nm. The concentrations of urea and creatinine were determined using some kids (BT Product, Turkey).

$$\text{Creatinine} + \text{Sodium Picrate} \xrightarrow{\text{Alkali}} \text{Creatinine - picrate complex (yellow - orange)}$$

Creatinine reacts with picric acid in alkaline conditions to form a color complex which absorbs at 510 nm. The rate of formation of color is proportional to the amount of creatinine in the sample.

$$\text{Urea} + H_2O \xrightarrow{\text{Urease}} 2\,NH_3 + CO_2$$

$$NH_3 + \alpha\text{ - Ketagluterate} + \text{NAD} \longrightarrow \text{L - Glutamate} + \text{NAD}$$

In the presence of water, urea is hydrolyzed by urease to produce ammonia and carbon dioxide. The liberated ammonia reacts with α-Ketagluterate in the presence of NADH to yield glutamate. An equimolar quantity of NADH undergoes oxidation during

the reaction resulting in a decrease in absorbance at 340 nm that is directly proportional to the urea nitrogen concentration in the sample.

In the case of urease immobilized membranes, the concentration of ammonia in the medium (decomposed urea) in both donor and receiver sides was determined by the method described in section 6.4. Then, urease was added into the solution to completely decompose the unreacted urea into ammonia. The concentration of urea in the solution was then determined from the difference in concentrations of ammonia measured before and after urea was decomposed completely with urease.

6.6. Characterization Studies

6.6.1. Measurement of Tensile Strength

The tensile strength of the membranes was measured using a Shimadzu AG-I-250 KN testing machine. The membranes were strained at a constant rates of 0.25 mm/min and 0.5 mm/min until failure. The test method and sample preparation was in accordance with ASTM D 882-02 standard. At least five test coupons with a 10 mm in width and 5 cm in length were used for measurements.

The tensile strength (δ) and the strain were calculated using the following equations:

$$\delta = \frac{F}{A} \tag{6.2}$$

$$\varepsilon = \frac{(L - L_0)}{L_0} \tag{6.3}$$

where, F is the applied load, A is the cross sectional area of the specimen, Lo is the original distance between gage marks and L is the distance between gage marks at any time. Young's modulus was obtained from the initial linear part of δ vs. ε graph.

6.6.2. Surface Characterization

The surface morphology of the membranes was examined by scanning electron microscopy (SEM) on a Philips XL-30SFG model. The samples were coated with gold using a Magnetron Sputter Coating Instrument.

CHAPTER 7

RESULTS AND DISCUSSION

7.1. Influence of Polymer Concentration on the Permeation of Solutes Through CA Membranes

The effect of changing the composition of the casting solution on the structure and separation performance of asymmetric-membranes is well documented. (Altinkaya and Ozbas 2004 , Altinkaya et al. 2005)

Table 7.1. Compositions of polymer, solvent and nonsolvent in the casting solution used to prepare different cellulose acetate (CA) membranes.

Code of the Membrane	Weight Percentage (%) of Three Components		
	Polymer (Cellulose Acetate)	Solvent (Acetone)	Nonsolvent (Water)
CAI	5	80	15
CAII	10	80	10
CAIII	15	80	5

To illustrate the relationship between the composition of the casting solution and permeation rates of solutes, the ratio of cellulose acetate (CA) to acetone was changed from 5/80 to 15/80 as shown in Table 7.1. Urea (M_w=60.06), creatinine (M_w=113.12) and uric acid (M_w=168.11) were chosen as model solutes since doctors usually decide if a patient should be connected to a hemodialysis unit or not based on the concentrations of these solutes in the blood. The initial concentrations of urea, uric acid and creatinine in the donor compartment were adjusted as 1000 mg/dl, 75 mg/dl and 100 mg/dl, respectively.

To determine the permeability coefficient of solutes from Equation 5.15 the difference in the concentrations measured in the donor and receiver compartments at different times, C_D-C_R, was normalized with respect to the initial concentration difference, C_{Di}-C_{Ri}. The change in the logarithm of this ratio, $ln\frac{C_D - C_R}{C_{Di} - C_{Ri}}$, as a function of time was plotted for

the permeation of each solute through all membranes prepared as shown in Figure 7.1. through Figure 7.9. Each data set in these figures was fitted to a linear equation and the quality of the fitted model was determined by high coefficient of determination, R^2 values, close to 1. The permeation coefficients were determined from Equation 5.15 by dividing the slope of the fitted data to a constant ß value of 0.59. In Figure 7.1 through Figure 7.9. three independent measurements were plotted and the permeation coefficients determined for each data set are listed in Table 7.2.

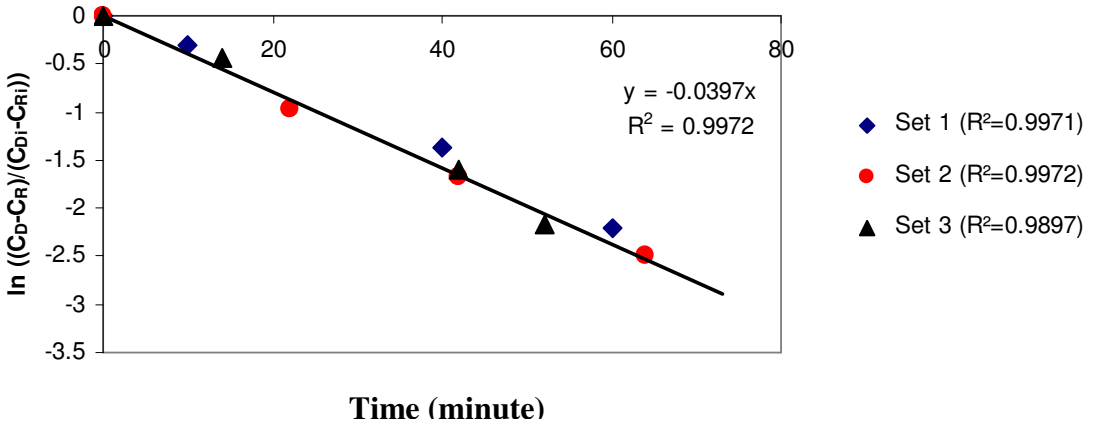

Figure 7.1. The change of $ln\frac{C_D - C_R}{C_{Di} - C_{Ri}}$ with respect to time for the permeation of urea through CAI membrane.

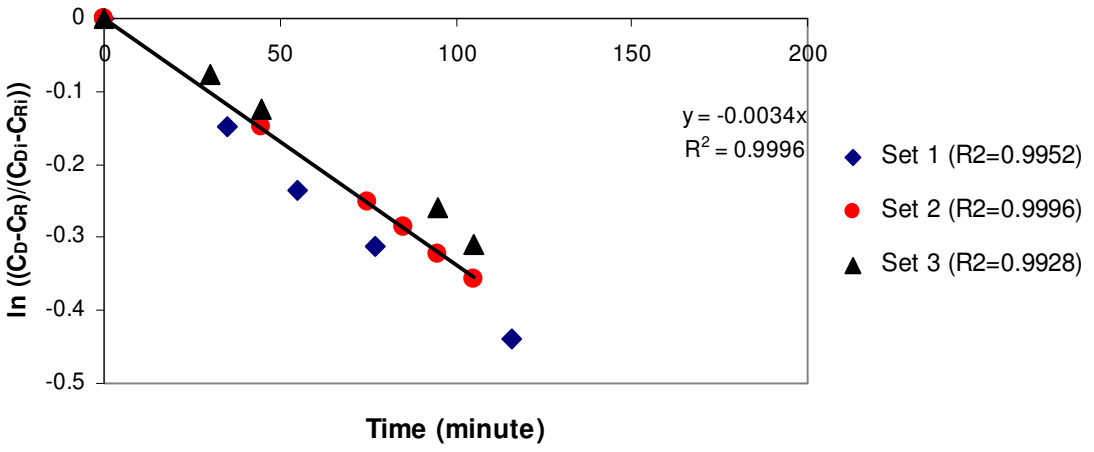

Figure 7.2. The change of $ln\frac{C_D - C_R}{C_{Di} - C_{Ri}}$ with respect to time for the permeation of uric acid through CAI membrane.

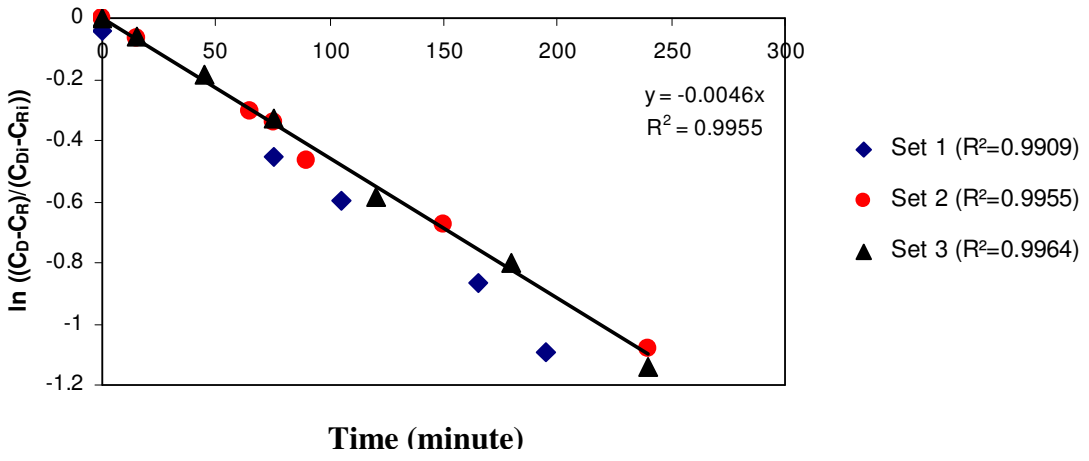

Figure 7.3. The change of $ln\frac{C_D - C_R}{C_{Di} - C_{Ri}}$ with respect to time for the permeation of creatinine through CAI membrane.

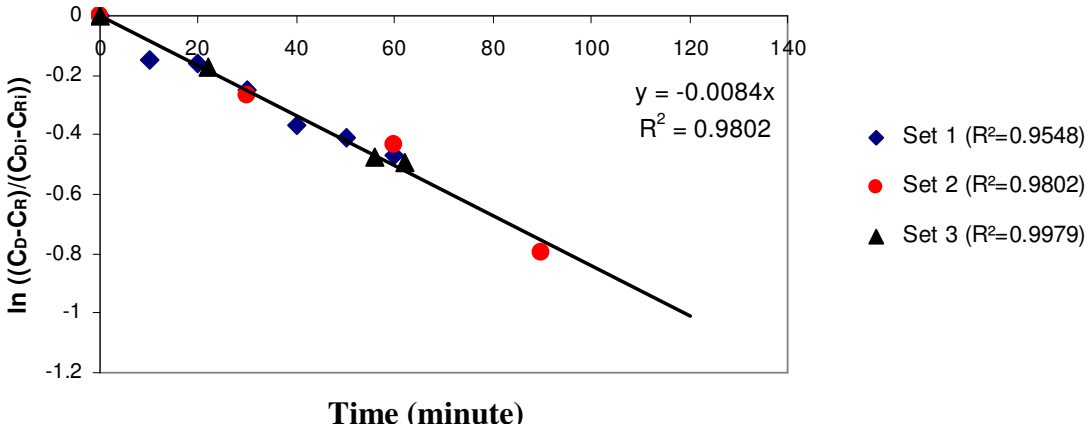

Figure 7.4. The change of $ln\frac{C_D - C_R}{C_{Di} - C_{Ri}}$ with respect to time for the permeation of urea through CAII membrane.

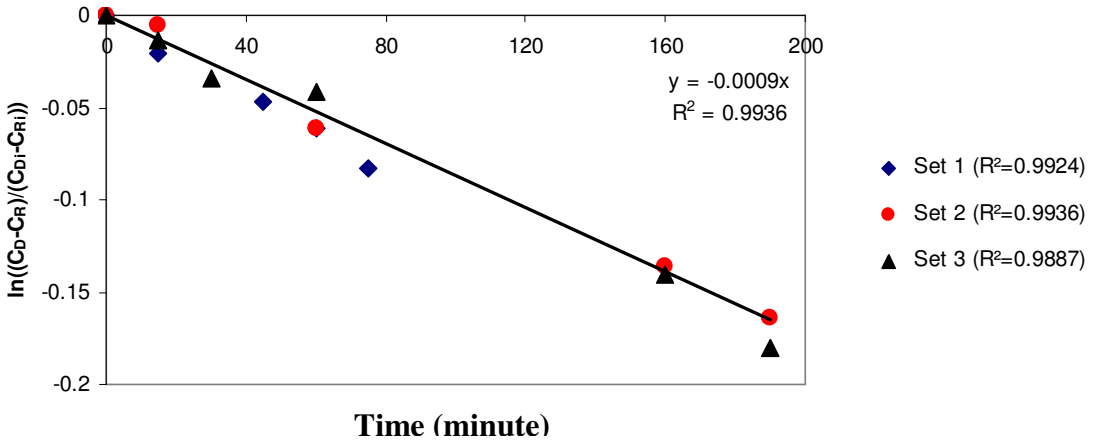

Figure 7.5. The change of $ln\frac{C_D - C_R}{C_{Di} - C_{Ri}}$ with respect to time for the permeation of uric acid through CAII membrane.

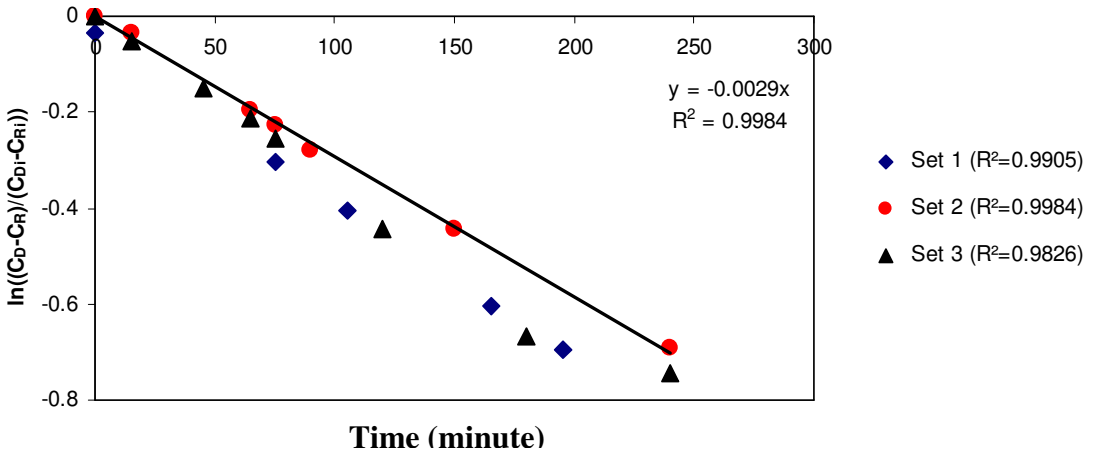

Figure 7.6. The change of $ln\frac{C_D - C_R}{C_{Di} - C_{Ri}}$ with respect to time for the permeation of creatinine through CAII membrane.

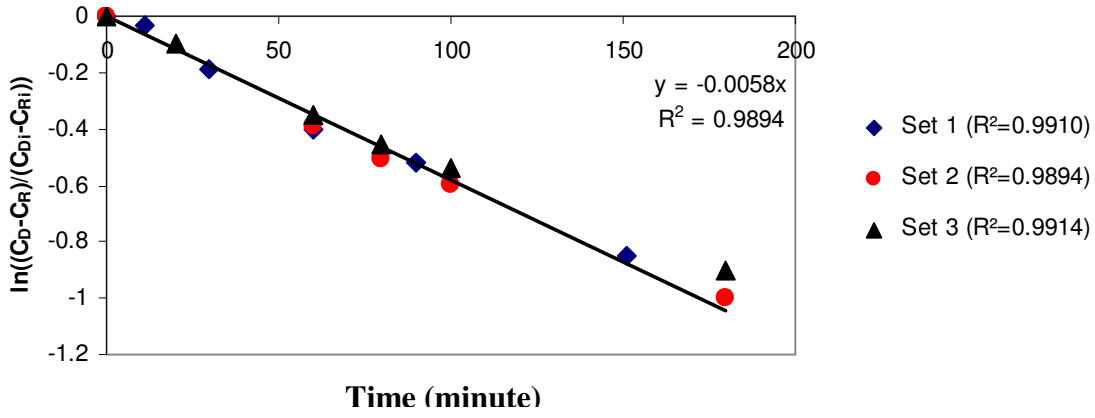

Figure 7.7. The change of $ln\frac{C_D - C_R}{C_{Di} - C_{Ri}}$ with respect to time for the permeation of urea through CAIII membrane.

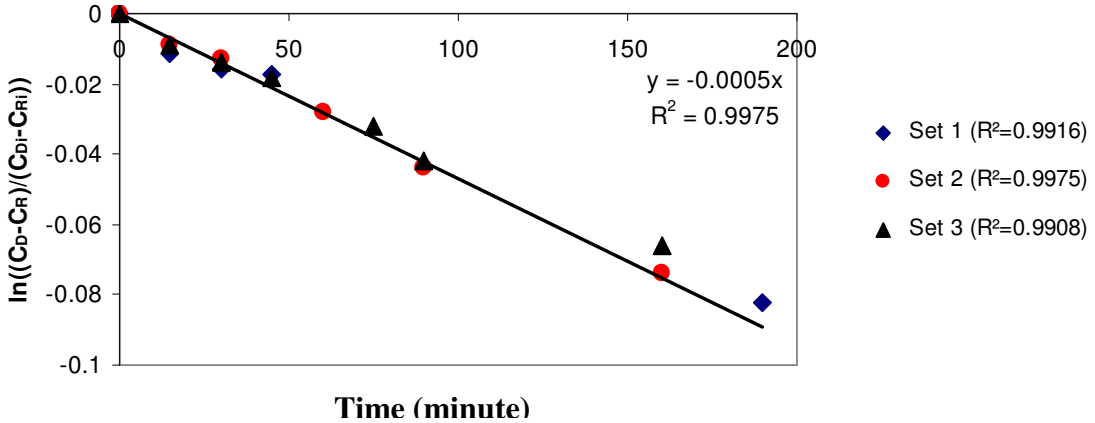

Figure 7.8. The change of $ln\frac{C_D - C_R}{C_{Di} - C_{Ri}}$ with respect to time for the permeation of uric acid through CAIII membrane.

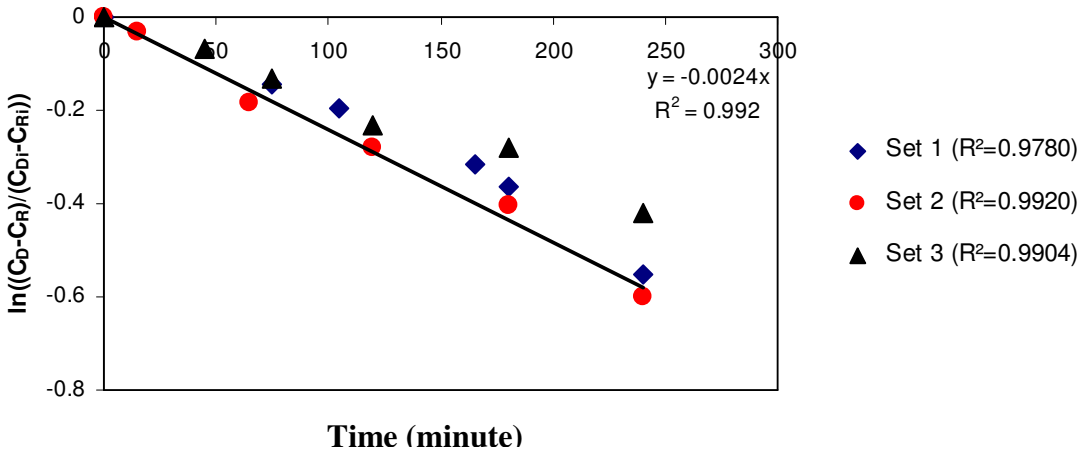

Figure 7.9. The change of $ln\frac{C_D - C_R}{C_{Di} - C_{Ri}}$ with respect to time for the permeation of creatinine through CAIII membrane.

Table 7.2. The permeation coefficients of three model solutes through CAI, CAII and CAIII membranes.

Solutes	M_w^* of Solutes	CAI					CAII					CAIII				
		Permeation Coefficient x 10^5 (cm/sec)					Permeation Coefficient x 10^5 (cm/sec)					Permeation Coefficient x 10^5 (cm/sec)				
		Set 1	Set 2	Set 3	Avg.**	STD***	Set 1	Set 2	Set 3	Avg.	STD	Set 1	Set 2	Set 3	Avg.	STD
Urea	60.06	104.40	112.90	101.30	**106.20**	**6.006**	23.50	23.80	23.20	**23.50**	**0.30**	16.41	16.41	14.70	**15.84**	**0.99**
Uric acid	168.11	11.04	9.62	9.53	**10.06**	**0.847**	3.11	2.55	2.55	**2.74**	**0.32**	1.13	1.41	1.13	**1.22**	**0.16**
Creatinine	113.12	15.56	11.21	11.21	**12.66**	**2.511**	10.47	8.21	9.62	**9.43**	**1.14**	5.94	4.81	6.79	**5.85**	**0.99**

* Molecular weight

** Average

*** Standard Deviation

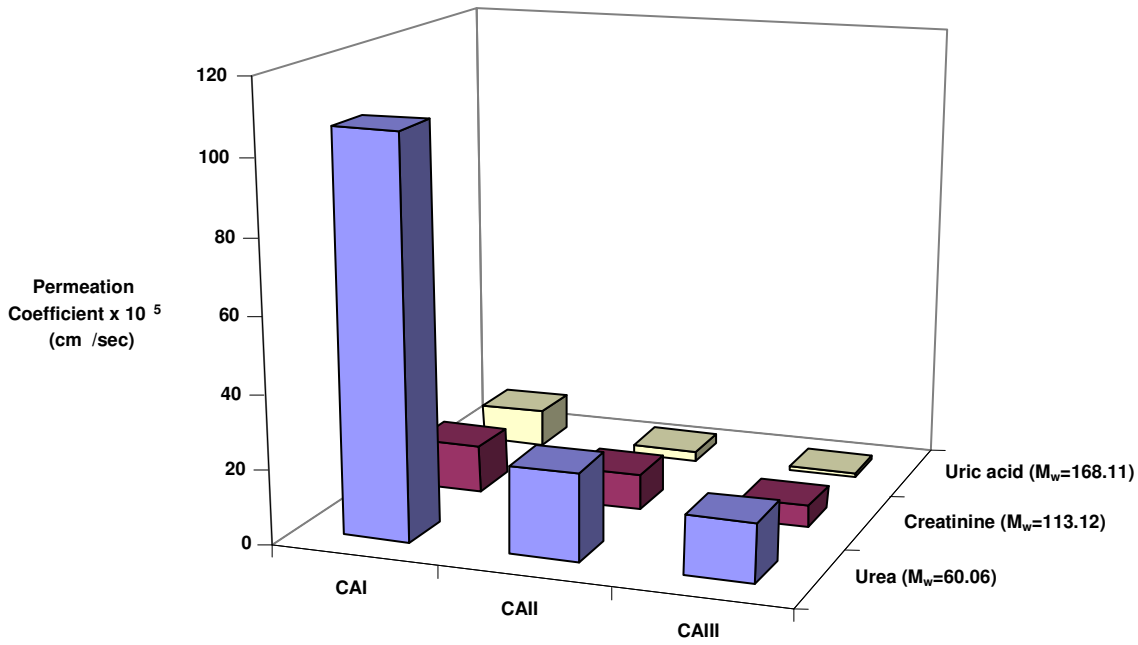

Figure 7.10. The permeation coefficients of three model solutes through CAI, CAII and CAIII membranes.

Figure 7.10 shows the change in averages permeation coefficients of each solute with the ratio of the CA to acetone concentrations in the initial casting solution. As expected, the permeation coefficient decreases exponentially with the increased molecular weight of the solutes. In addition, the permeation coefficient of each solute decreases in a similar way as the concentration of CA in the initial casting solution increases from 5% to 15%. This is mainly caused by the final structures of the membranes as shown in Figure 7.11 through Figure 7.13. Structural parameters obtained from the scanning electron microscope (SEM) pictures of the membranes are listed in Table 7.3.

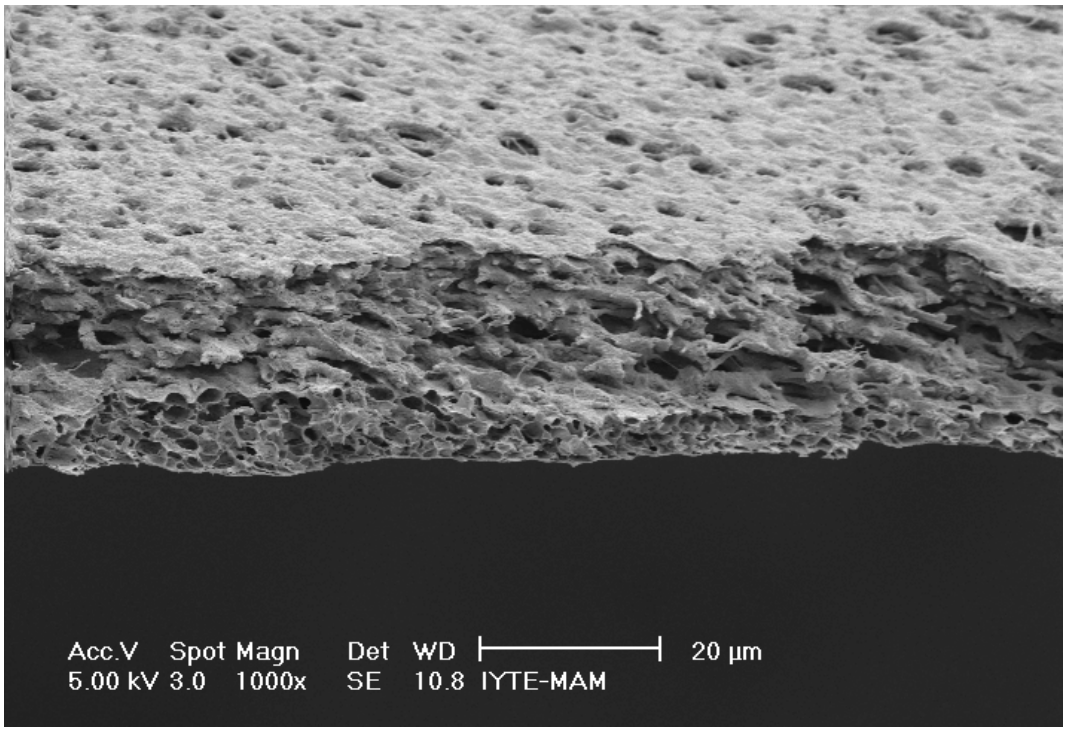

Figure 7.11. SEM picture of CAI membrane, magnification 1000x.

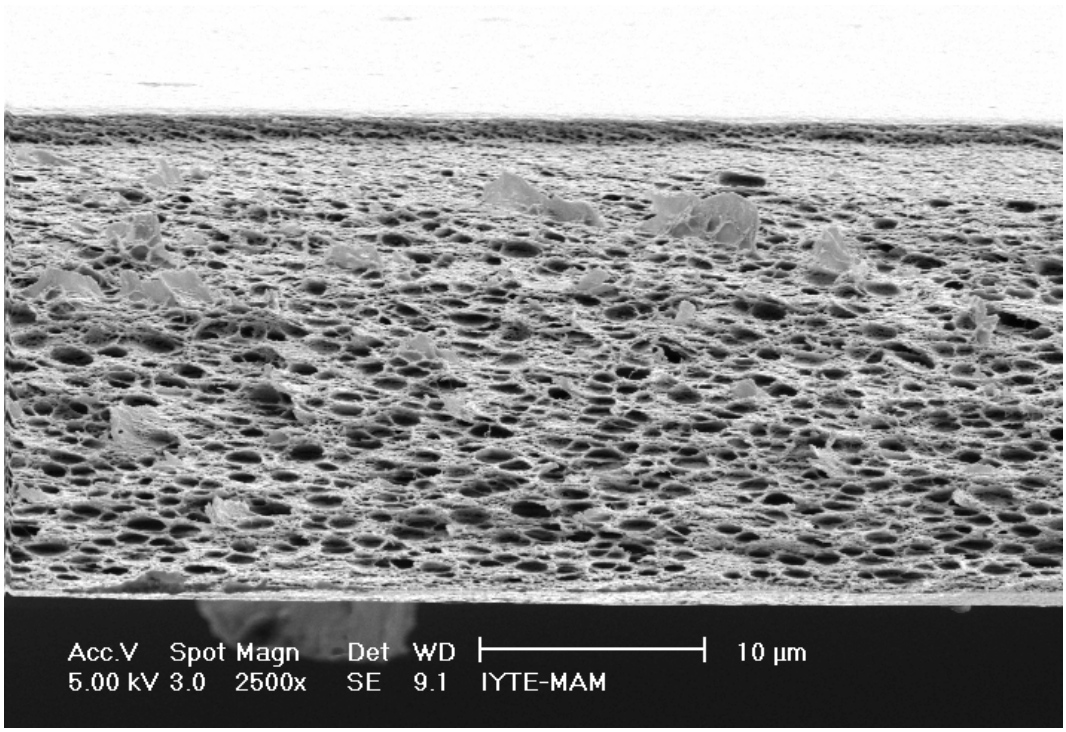

Figure 7.12. SEM picture of CAII membrane, magnification 2500x.

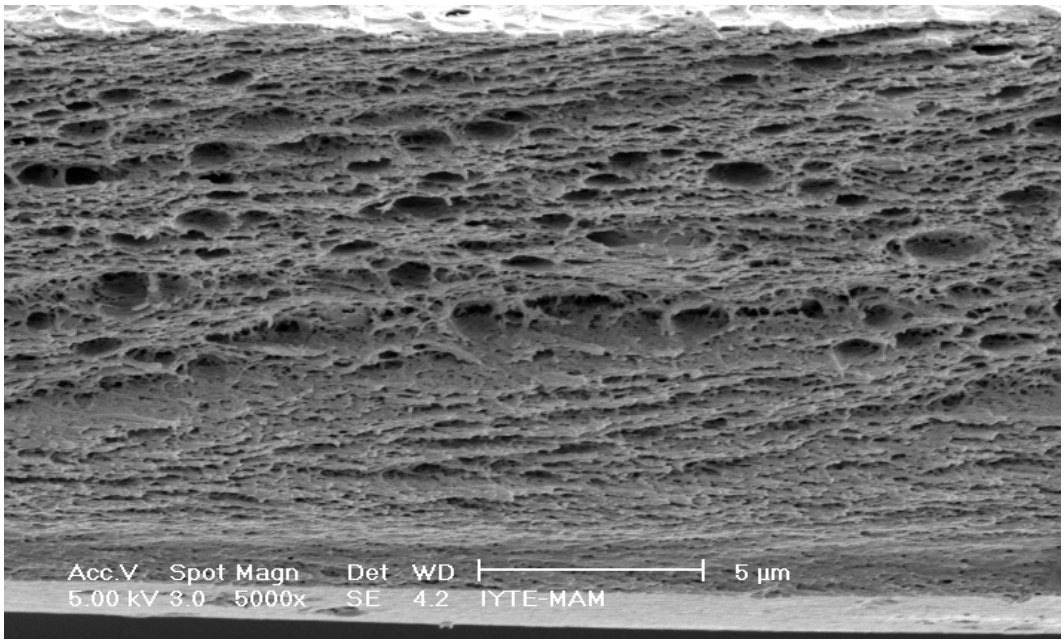

Figure 7.13. SEM picture of CAIII membrane, magnification 5000x.

Table 7.3. Morphological characteristics of CAI, CAII, CAIII membranes.

Membrane	Polymer Content (wt %)	Thicknes of Membrane (µm)	Percentage of Dense Skin Layer (%)	Average Pore Size (µm)
CAI	5	27.94	13.44	1.15
CAII	10	19.69	17.10	0.53
CAIII	15	19.16	29.96	0.42

It can be seen from the results that with the increased CA concentration in the solution, the average pore sizes decrease while the percentage of dense skin layer increases significantly which causes a reduction in the transport rates of solutes. CAI membrane prepared with 5% CA in the casting solution is thicker than those prepared with 10% and 15% CA concentrations. This result is explained by the presence of macrovoids as shown in Figure 7.11. Macrovoid formation in dry cast CA membranes was reported by some other groups (Pekny et al. 2002, 2003). Even though macrovoid

formation is not well understood, it is usually attributed to the buoyancy and gravity effects (Pekny et al. 2003).

7.2. Characterization of Urease Immobilized Cellulose Acetate Membranes.

7.2.1. Determination of Stability of Immobilized Urease Activities

The stability of immobilized urease activities was determined in both wet and dry conditions. Figure 7.14. shows the change in the relative activity of immobilized urease when the CA membrane was stored at 37C° in a pH 7.4 phosphate buffer solution. Activity was measured during 4 hours of time period which corresponds to typical hemodialysis time. Approximately 30% of the initial activity was lost within 3 hours and 18% of the activity was recovered within the next 1 hour. Recovery in the lost activity may be attributed to a change in the conformation of the immobilized enzyme so that more active site of the enzyme becomes available for the decomposition of urea.

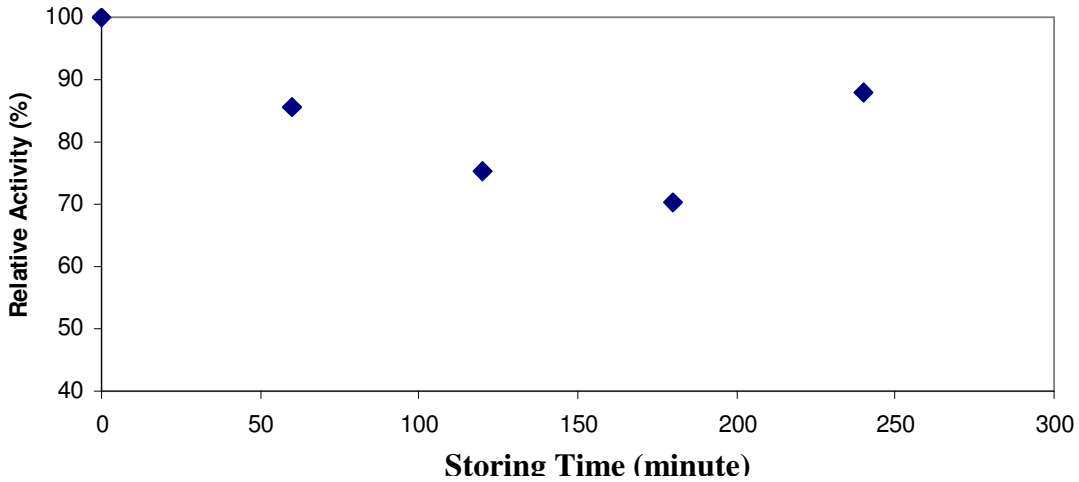

Figure 7.14. The effect of storing time on the relative activity of urease immobilized in CAI membrane. Initial activity of urease=1.18 micromole NH_3 / min x cm². Membrane was stored in phosphate buffer solution at pH=7.4, T=37°C.

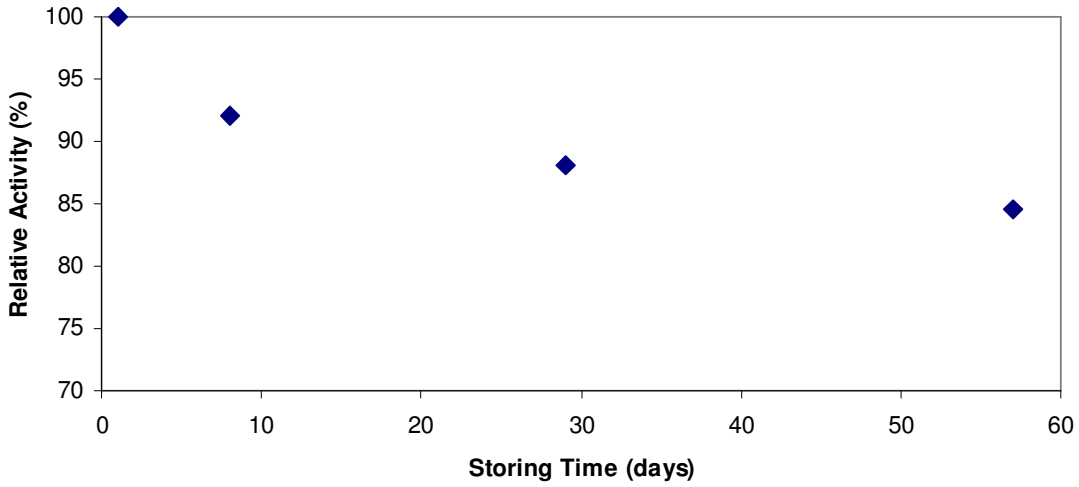

Figure 7.15. The effect of storing time on the relative activity of urease immobilized in CAI membrane. Initial activity of urease=1.18 micromol NH_3 / min x cm². Membrane was stored in dry form at 4°C.

Figure 7.15. shows the change in immobilized urease activity when CAI membrane was stored at 4C° in a dry form. According to this figure, dry-stored immobilized urease retained its activity above 85% for almost 60 days. The activity of dry-stored urease is much higher than that of wet-stored urease, since dry storage temperature is lower than that of wet storage temperature. In addition, phosphate buffer solution contributes to the faster inactivation of urease. Similar results were reported in the literature by some other groups. Krajewska et al. (1990) reported 30% lost in the initial activity of wet-stored immobilized urease within 10 days and 20% lost over a period of 60 days when immobilized urease was stored in a dry form. Lin and Yang (2003) found that dry-stored cholesterol oxidase (COD) retained its activity above 95% for 60 days, while the activity in wet form decreased sharply when it was stored for more than 3 days. The stability of immobilized urease in dry form during storage is an important factor for their economical use in commercial hemodialysis units.

7.2.2. Determination of Kinetic Parameters of Immobilized Urease

Enzyme kinetics are usually described by the well known Michaelis-Menten equation as shown by Equation 5.19. The values of K_m and V_{max} can be easily determined by using the reciprocal of Equation 5.19.

$$\frac{1}{V} = \frac{K_m}{V_{max} \times [S]} + \frac{1}{V_{max}} \qquad (7.1)$$

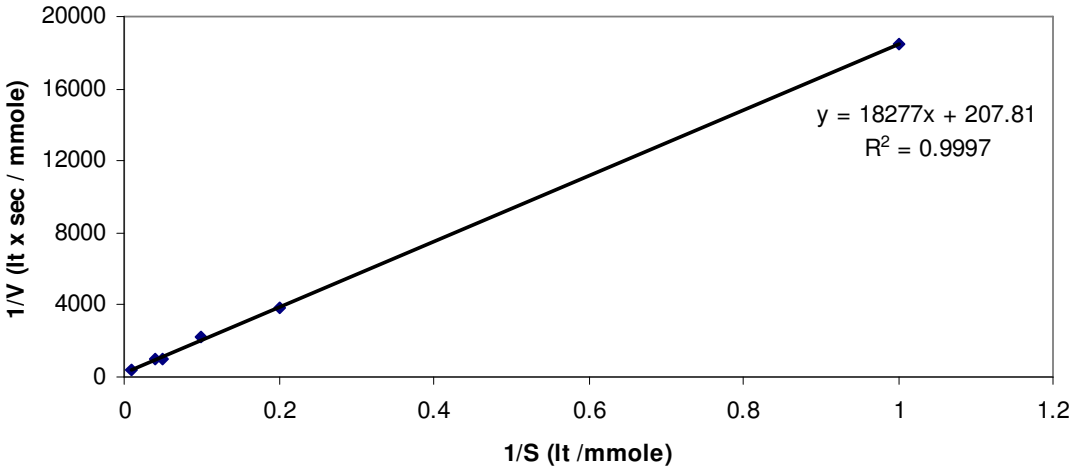

Figure 7.16. Kinetic parameters of urease immobilized CA membrane.

The reciprocal of the rate of reaction (1/V) plotted as a function of the reciprocal of the initial substrate concentration (1/S) is shown Figure 7.16. A linear relationship between (1/V) and (1/S) indicated by high R^2 value close to 1 demonstrates that the decomposition of urea by the urease immobilized membrane follows the Michaelis-Menten type kinetics. The Michaelis constant K_m and the maximum rate of reaction, V_{max}, determined from the slope and intercept of the plot in Figure 7.16 are listed in Table 7.4. Kinetic parameters of the native urease were also reported in the same table.

Table 7.4. Kinetic data for decomposition urea by native urease and urease immobilized CA membrane.

	V_{max} (mmol/sec x lt)	**K_m (mM)**
Native Urease	0.0103	13.7
Urease immobilized CA membrane	0.0048	87.9

In Equation 7.1, the K_m value indicates the affinity of an enzyme to its substrate, while V_{max} represents the maximum rate of reaction. The increase of K_m value with the

immobilization of urease indicates a lower affinity between urease and urea than that of the soluble, native urease (Uragami et al. 2003). On the other hand, V_{max} of the urease-immobilized CA membrane is almost half of the V_{max} of the native urease. This is due to inactivation of urease during immobilization and increased diffusional resistance encountered by the urea while it approaches to the catalytic site.

7.3. Permeation of Solutes Through Urease Immobilized Cellulose Acetate Membranes

Urease immobilized CA membrane was prepared by blending urease directly into the CA casting solution which consisted of 5% CA, 80% acetone, 0.5% urease and 14.5% deionized water. To determine the influence of urease immobilization on the solute transport rates, permeation experiments for three model compounds were performed with the same initial concentrations used in the previous experiments. Figure 7.17. and Figure 7.18. show the plot of $ln\frac{C_D - C_R}{C_{Di} - C_{Ri}}$ as a function of time for three sets of independent measurements. Permeation coefficients of uric acid and creatinine in urease immobilized CA membrane were directly determined from equation 5.15 and they are listed in Table 7.5.

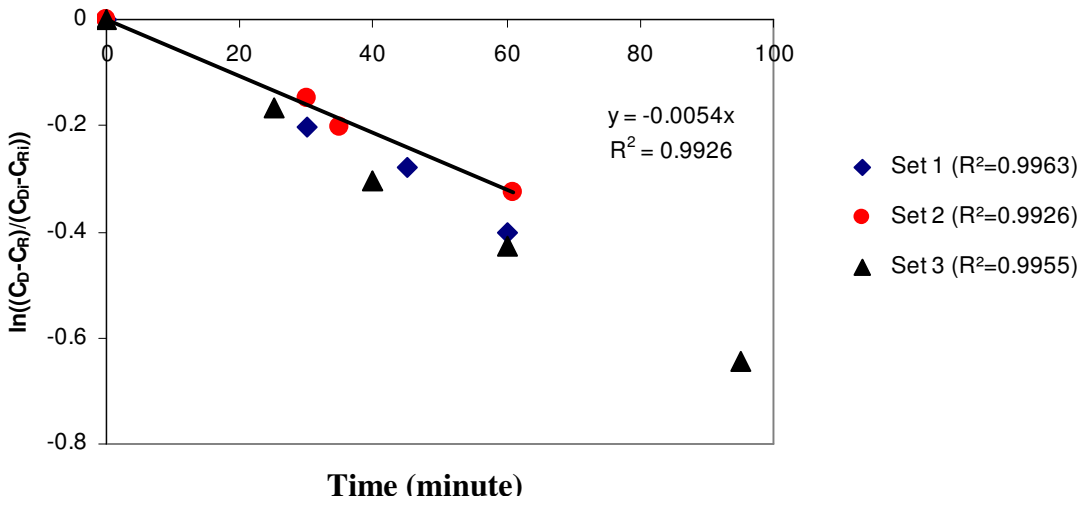

Figure 7.17. The change of $ln\frac{C_D - C_R}{C_{Di} - C_{Ri}}$ with respect to time for the permeation of uric acid through urease immobilized CA membrane.

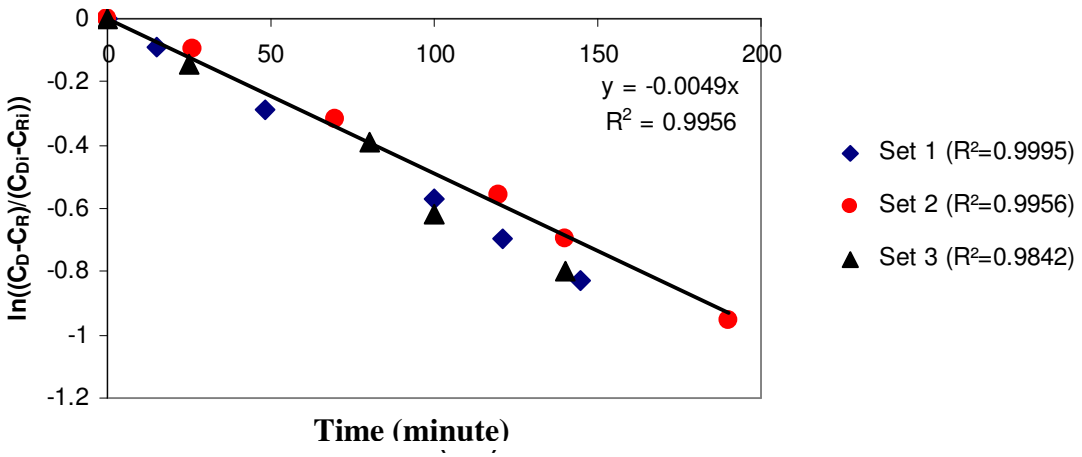

Figure 7.18. The change of $ln\frac{C_D - C_R}{C_{Di} - C_{Ri}}$ with respect to time for the permeation of creatinine through urease immobilized CA membrane.

Table 7.5. Permeation coefficient of two solutes through urease immobilized CA membrane and regular CA membrane.

Solutes	**M_W* of Solutes**	**Urease Immobilized CA Membrane**					**CAI Membrane**
		Permeation Coefficient x 10^5 (cm/sec)					**Permeation Coefficient x 10^5 (cm/sec)**
		Set 1	**Set 2**	**Set 3**	**Avg.****	**STD*****	**Avg.**
Creatinine	113.12	16.10	13.90	16.10	**15.37**	**1.2702**	12.66
Uric acid	168.11	18.70	15.30	19.50	**17.83**	**2.2301**	10.06

* Molecular weight

** Average

*** Standard Deviation

The results clearly indicate that permeation coefficients of both uric acid and creatinine increased through urease immobilized CA membrane. This observation is explained by the change in the structure as shown in Figure 7.19. The comparison of the scanning electron micrographs shown in Figure 7.11 and Figure 7.19 indicate that the fraction of dense skin layer decreases significantly and due to the absence of

macrovoids, the membrane becomes thinner by adding urease into the casting solution. Structural parameters of these two membranes are listed in Table 7.6.

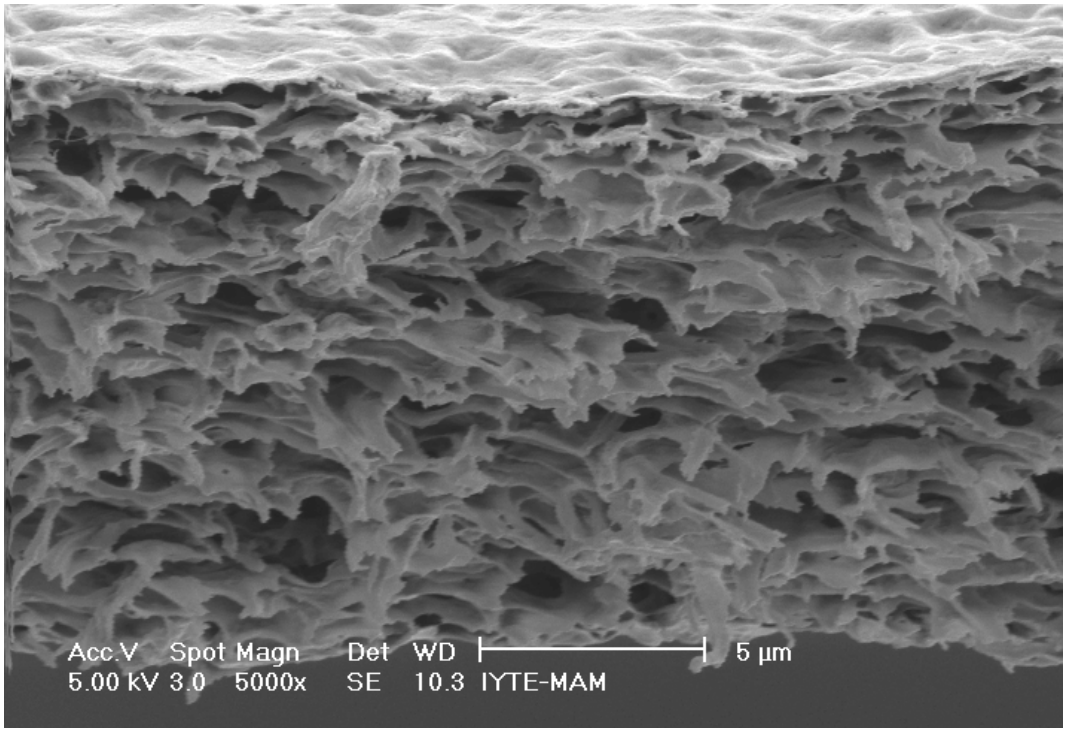

Figure 7.19. SEM picture of urease immobilized CA membrane, magnification 5000x.

Table 7.6. Comparison of morphological characteristics of urease immobilized and regular CA membranes.

Membrane	**Polymer Content (%)**	**Thicknes of Membrane (µm)**	**Percentage of Dense Skin Layer (%)**	**Average Pore Size (µm)**
CAI	5	27.94	13.44	1.15
Urease Immobilized CA Membrane	5	16.71	2.62	1.37

Figure 7.20a and 7.20b show the comparison of the change in the urea concentration in the donor and receiver compartments when CAI and urease immobilized CA membranes were used. An increase in the urease concentration in the casting solution while keeping the

polymer concentration constant as 5% enhanced the removal of urea. The % removal of urea from the donor compartment within 1 hour was calculated as 45.8%, 53.2% and 68.4% for CAI, 0.5% urease immobilized CA and 2% urease immobilized CA membranes, respectively. The results clearly indicate that amount of urease blended into the membrane forming solution is an important parameter to increase the benefit of using urease immobilized membranes for the hemodialysis operation.

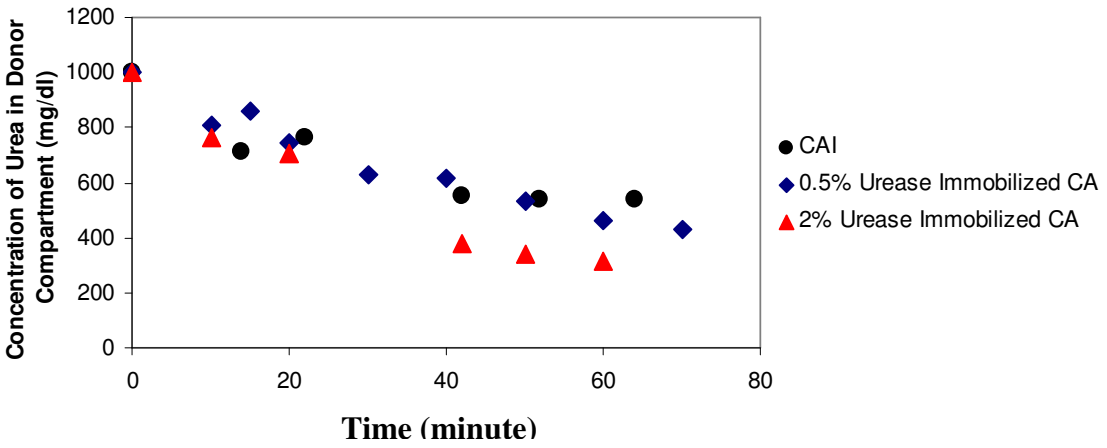

(a)

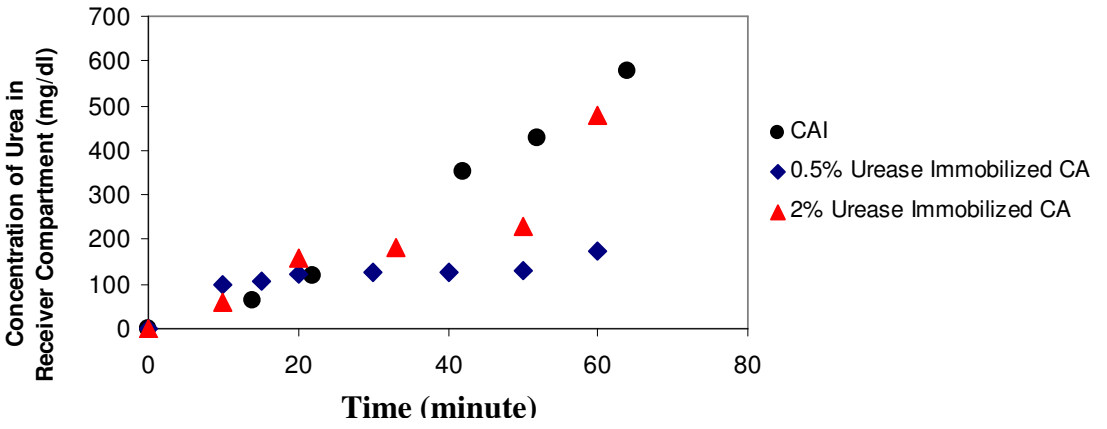

(b)

Figure 7.20. The change of concentration of urea in a) donor b) receiver compartments with respect to time when regular CA and urease immobilized CA membranes were used.

To model the rate of removal of urea from the donor compartment using urease immobilized membrane, the model equations shown in Equations 5.19 through 5.33

were used. The model was applied for the case of 0.5% urease immobilized membrane. The input parameters used in the model are listed in Table 7.7.

Table 7.7. Input parameters used in the mathematical model shown by Equations 5.19 through 5.33.

Parameter	**Value**
K_m (mmol/lt)	87.9
V_{max} (mmol/sec x lt)	0.0048
K	18576.4
Thickness of the membrane (cm)	0.0016
Diffusivity of urea in the membrane (cm²/sec)	9.5×10^{-11}

K_m and V_{max} values reported in Table 7.7. were determined from enzyme kinetic measurements as discussed in section 7.2.2., while the partition coefficient, K, was determined by immersing a piece of membrane into the urea solution until equilibrium was achieved. Diffusivity of urea in the membrane was repressed from the experimental data by minimizing the following objective function.

$$\sum_{i=1}^{N_{data}} \left[\left(C_{D_{\exp}} - C_{D_{\mathrm{mod}\,el}} \right)^2 + \left(C_{R_{\exp}} - C_{R_{\mathrm{mod}\,el}} \right)^2 \right] \tag{7.2}$$

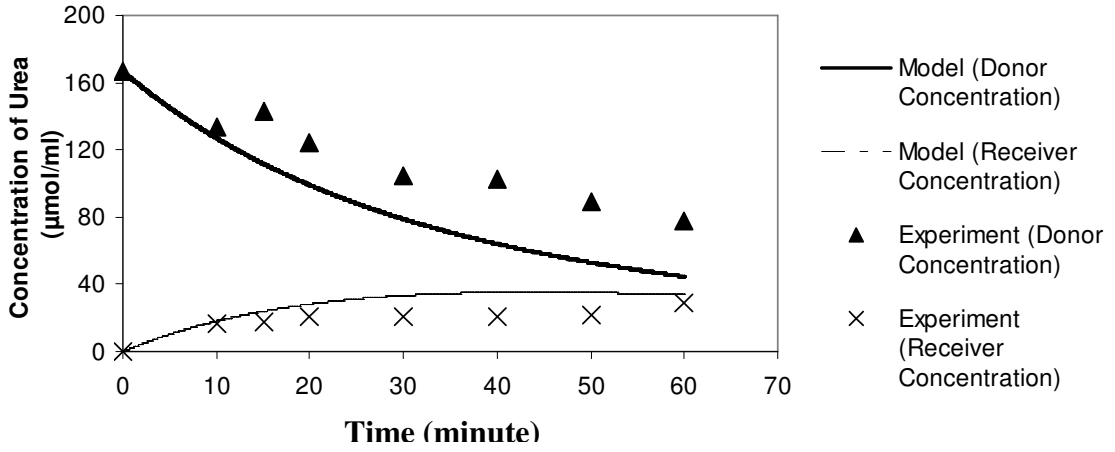

Figure 7.21. Comparison of model predictions with the experimental data for the concentration of urea in both donor and receiver compartments.

Figure 7.21. shows the comparison between the model predictions and experimental measurements for urea concentration in the donor and receiver compartments. The model prediction for the concentration of urea in the donor compartment is lower than that of the experimental data; in other words the model predicts a higher rate of removal of urea from the donor compartment. This is due to the combined effects of two facts that the model does not take into account the inactivation of enzyme and inhibition of product on the rate of reaction.

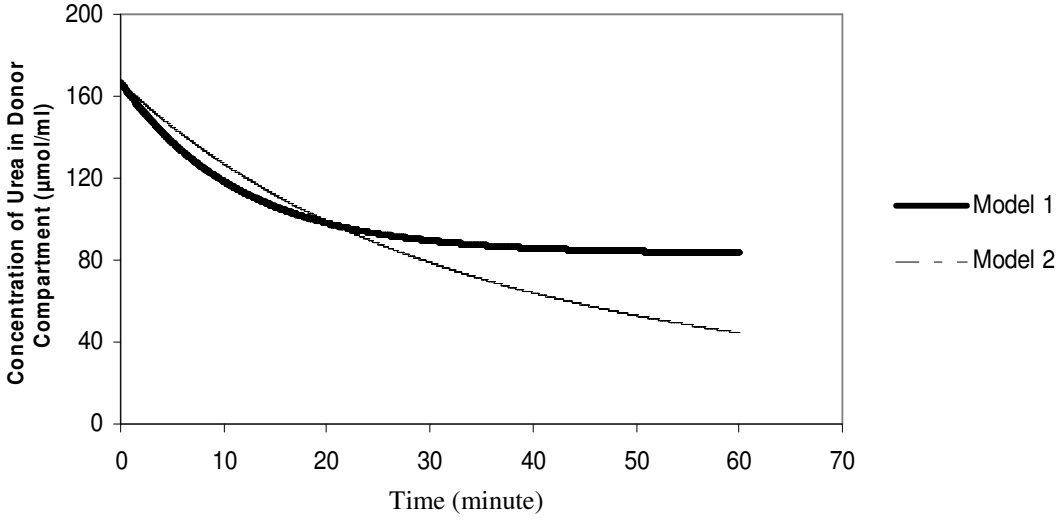

Figure 7.22. Predictions of concentration of urea in the donor compartment. Model 1 gives the urea concentration when regular CA membrane is used, while model 2 predicts the urea concentration when urease immobilized CA membrane is used.

The advantage of urease immobilized CA membrane over regular CA membrane for the rate removal of urea is illustrated in Figure 7.22. based on the model predictions. Model 1 and model 2 predict the concentration of urea in the donor compartment when the regular CA membrane and the urease immobilized CA membrane are used, respectively. Within the first 20 minutes, both models predict similar urea concentrations in the donor compartment indicating that the rate of removal of urea within this period is mainly controlled by diffusion of urea through the membrane. After 20 minutes from the beginning of the permeation process, model 2 predicts lower urea concentration in the donor compartment; since in this region; rate of transfer of urea

through the membrane is governed by the decomposition of urea using the immobilized urease.

A dimensionless parameter called as Thiele modulus can give a measure of diffusion and reaction limitations as follows (Giorno and Drioli 2000):

$$\text{Ø} = \text{L} \times \left(\frac{\text{V}_{\max}}{\text{D}_{\text{eff}} \times K_m} \right)^{\frac{1}{2}} \tag{7.3}$$

where L is the thickness of the membrane and D_{eff} is the effective diffusivity. The Thiele modulus compares the reaction rate and diffusion rate. If Ø <= 1, transport of solute is essentially controlled by the reaction and mass transfer limitation is negligible. Using the values in Table 7.7., Thiele modules was calculated as 1.72 indicating that transport of urea through urease immobilized CA membrane is governed both by its diffusion and decomposition. This conclusion is confirmed by the predictions shown in Figure 7.22.

7.4. Permeation of Solutes Through Protein Fouled Cellulose Acetate Membranes

To determine the influence of protein fouling on the transport rates of the solutes, permeation experiments were repeated with the regular and urease immobilized CA membranes both of which were prepared with 5% CA in the casting solution, and the latter one was modified by blending 0.5% urease into the solution. Protein adsorption capacity of each membrane was determined by following the decrease in the concentration of bovine serum albumin (BSA) in the solution. It was found that the membranes saturated with the BSA within 24 hours of period.

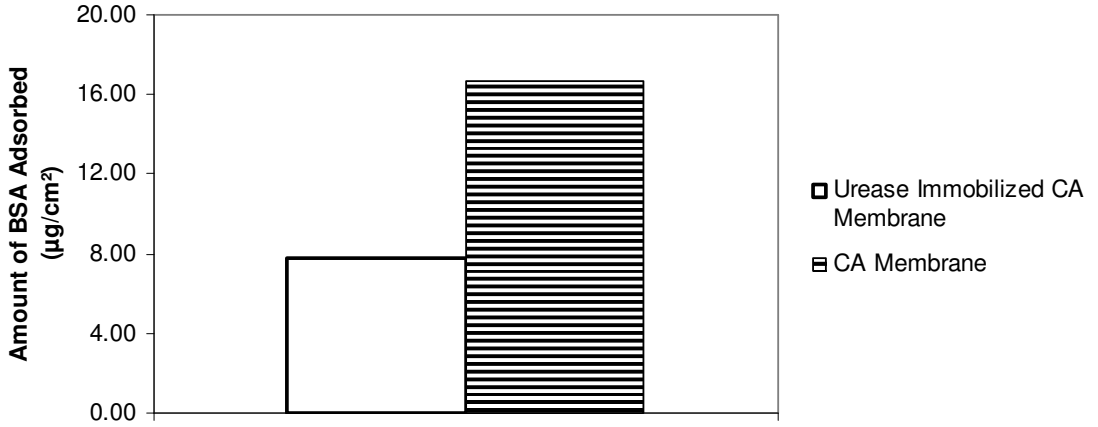

Figure 7.23. Amount of BSA adsorbed on cellulose acetate and urease immobilized cellulose acetate membranes.

Figure 7.23. shows that amount of BSA adsorbed on the regular CA membrane and urease immobilized CA membranes are 16.7 µg/cm² and 7.8 µg/cm², respectively. Protein adsorption capacity of CA membrane was decreased by a factor of 2.2 through urease immobilization. This observation can be explained by the change in surface hydrophilicity of CA membrane. During protein adsorption experiments, pH of the BSA solution was adjusted the same as the pH of the blood (pH=7.4). Isoelectric points of urease enzyme and the BSA are 5 and 4.9, respectively, thus , at pH=7.4, both of them are negatively charged. Due to electrostatic interactions, urease enzyme located on the surface of the membrane repels BSA, consequently, amount of BSA adsorbed on the urease immobilized membrane decreases.

The results of permeation experiments for uric acid and creatinine through BSA fouled CA membranes are shown in Figure 7.24. through Figure 7.27. Three sets of independent measurements were plotted in these figures and permeabilities were calculated from the slope of each data set.

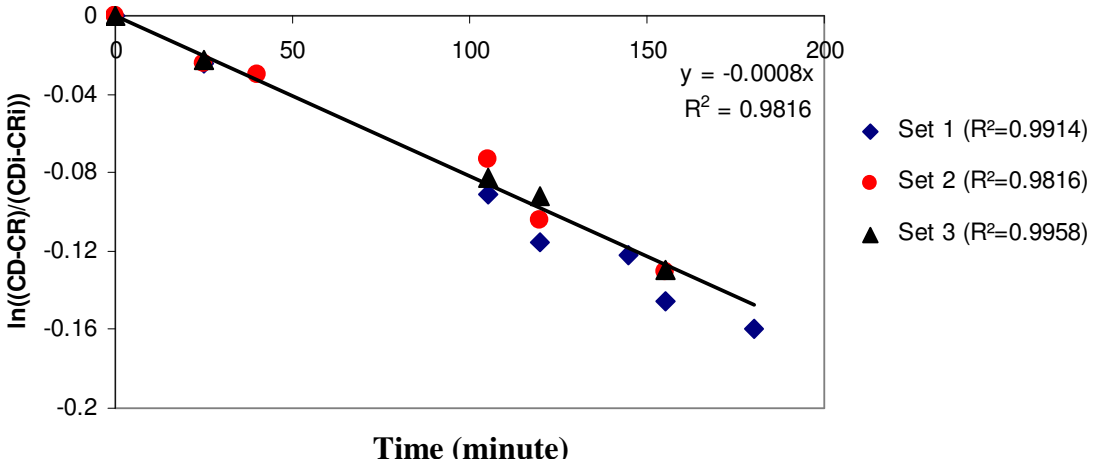

Figure 7.24. The change of $ln\frac{C_D - C_R}{C_{Di} - C_{Ri}}$ with respect to time for the permeation of uric acid through BSA fouled CAI membrane.

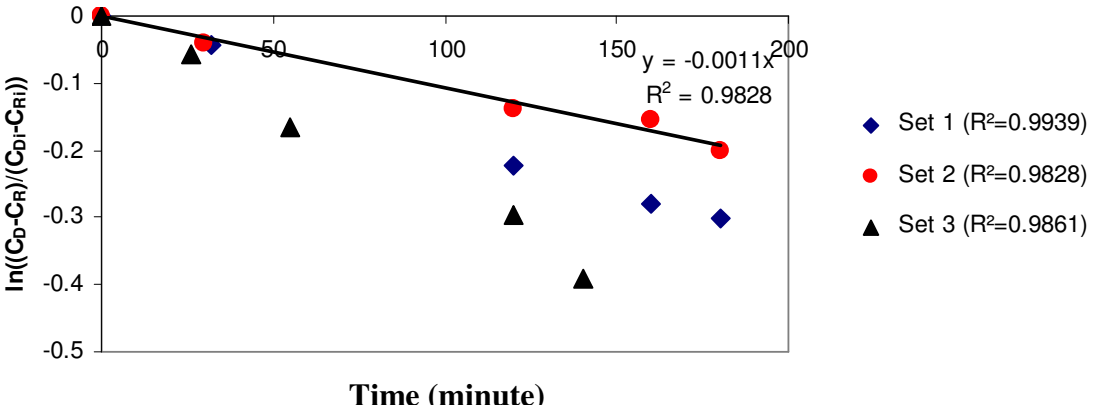

Figure 7.25. The change of $ln\frac{C_D - C_R}{C_{Di} - C_{Ri}}$ with respect to time for the permeation of creatinine through BSA fouled CAI membrane.

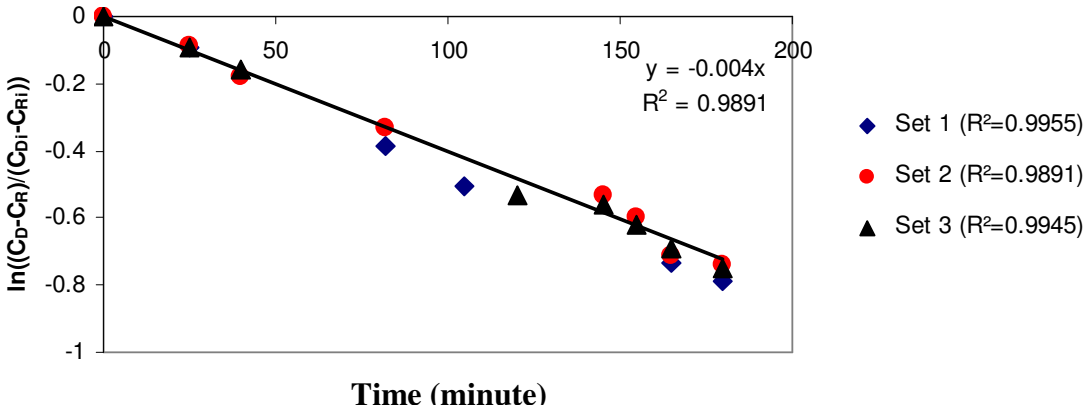

Figure 7.26. The change of $ln\frac{C_D - C_R}{C_{Di} - C_{Ri}}$ with respect to time for the permeation of uric acid through BSA fouled urease immobilized CA membrane.

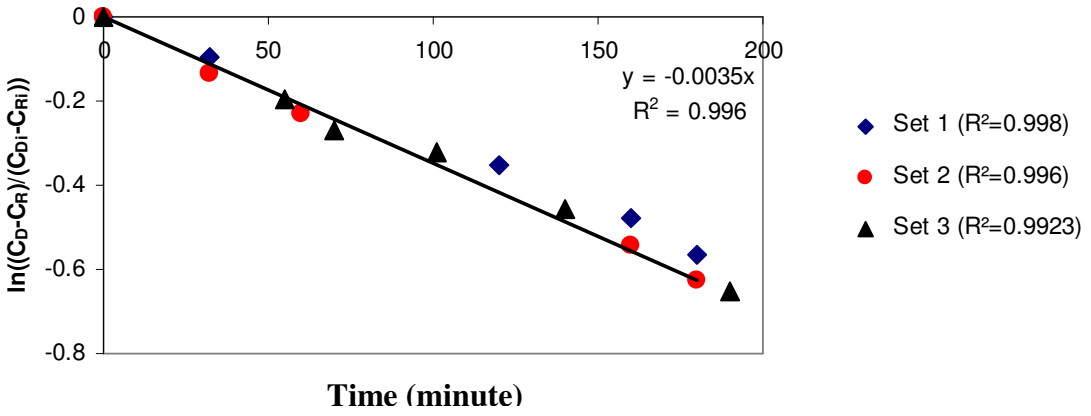

Figure 7.27. The change of $ln\frac{C_D - C_R}{C_{Di} - C_{Ri}}$ with respect to time for the permeation of creatinine through BSA fouled urease immobilized CA membrane.

The average permeabilities of uric acid and creatinine through regular CA and urease immobilized CA membranes fouled with BSA are shown in Figure 7.28 and Figure 7.29 respectively. For a comparison, the permeation coefficients of both solutes through clean membranes were also plotted in these figures.

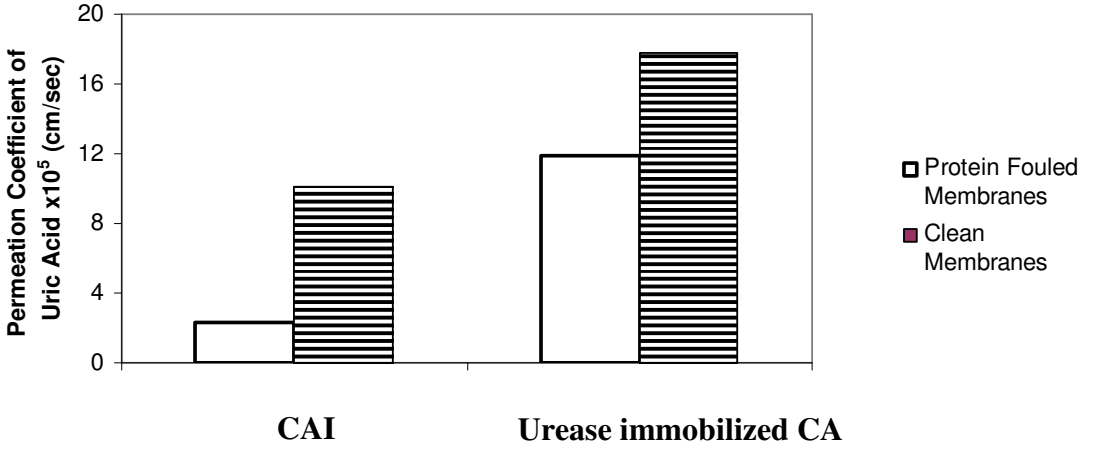

Figure 7.28. The change of permeation coefficient of uric acid due to protein fouling on CAI and urease immobilized CA membranes.

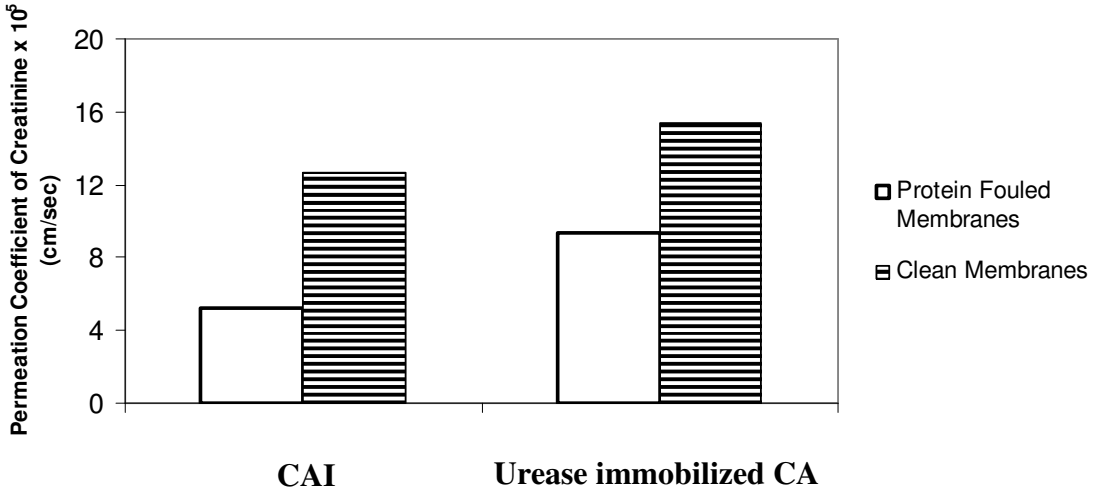

Figure 7.29. The change of permeation coefficient of creatinine due to protein fouling on CAI and urease immobilized CA membranes.

As expected, protein fouling on the membranes caused a decrease in the permeation coefficients of both solutes. The decrease in the permeation coefficient of creatinine through regular CA and urease immobilized CA membranes are calculated as 59.0% and 39.2%, respectively. Similarly, protein fouling caused a decrease in the permeation coefficient of uric acid through regular CA and urease immobilized CA membranes by 76.5% and 33.4%, respectively. The results clearly indicate that; modification of CA membrane with urease immobilization cannot completely eliminate protein adsorption problem, however, this strategy leads to a lower decline in the

transport rates of both uric acid and creatinine by limiting the protein adsorption capacity of CA membranes. Similarly, the change in the concentration of urea in both donor and receiver compartments were followed when protein fouled CA membrane and urease immobilized CA membrane were used. The results shown in Figure 7.30a and 7.30b indicate that rate of removal of urea from the donor compartment is faster in the case of urease immobilized CA membrane even if the membranes were fouled with BSA.

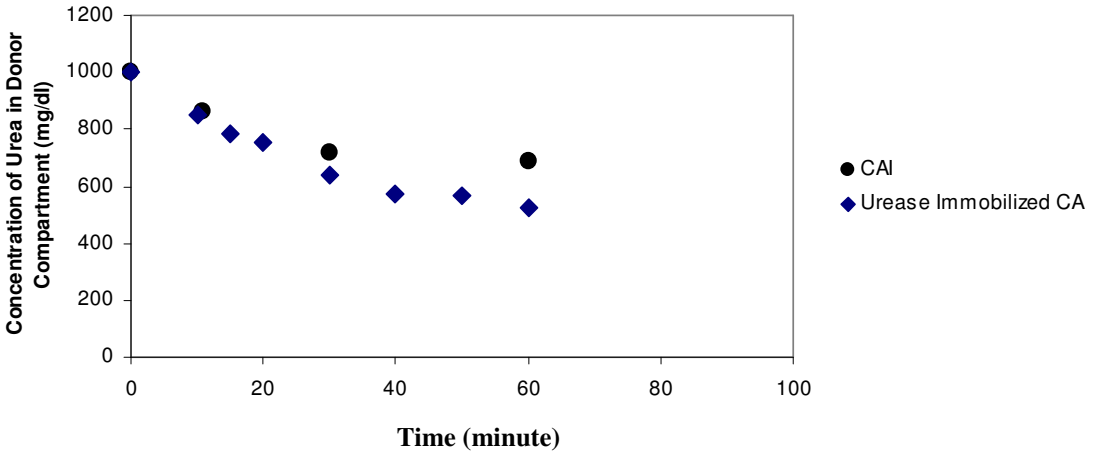

(a)

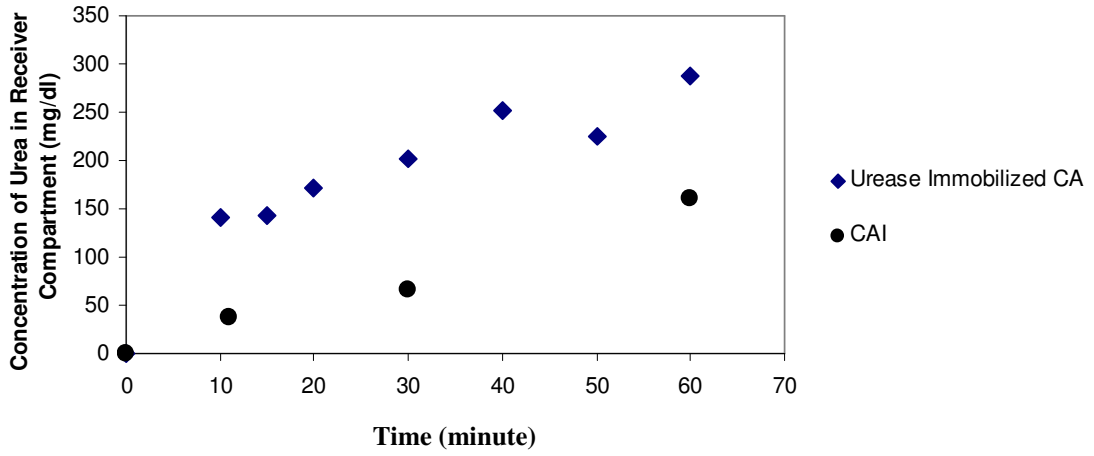

(b)

Figure 7.30. The change of concentration of urea in a) donor b) receiver compartments with respect to time when BSA fouled regular CA and urease immobilized CA membranes were used.

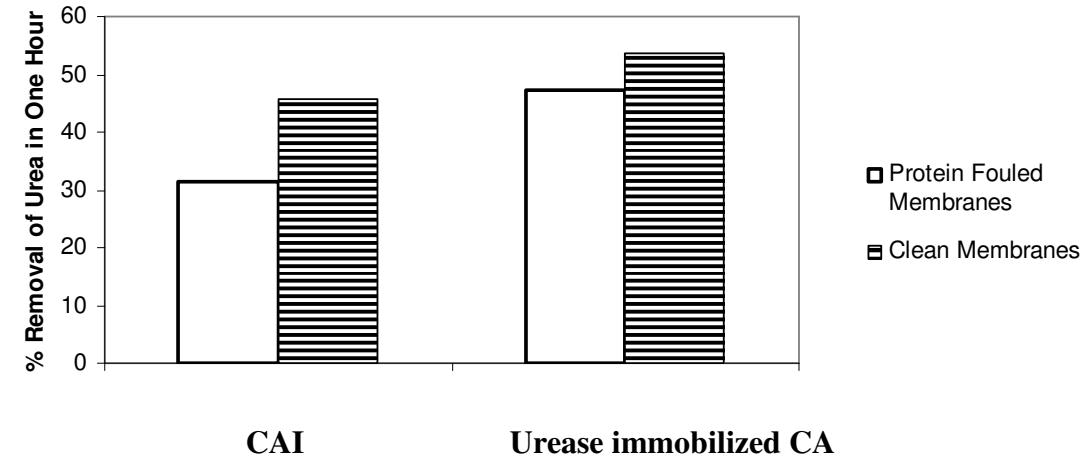

Figure 7.31. The change of % removal of urea due to protein fouling on CAI and urease immobilized CA membranes.

Figure 7.31 shows that due to protein fouling the rate of removal of urea from the donor compartment in one hour decreased by 31.2% and 11.7% through regular CA membrane and urease immobilized CA membrane, respectively. Urease immobilization technique also limited the decrease in the removal of urea due to protein fouling.

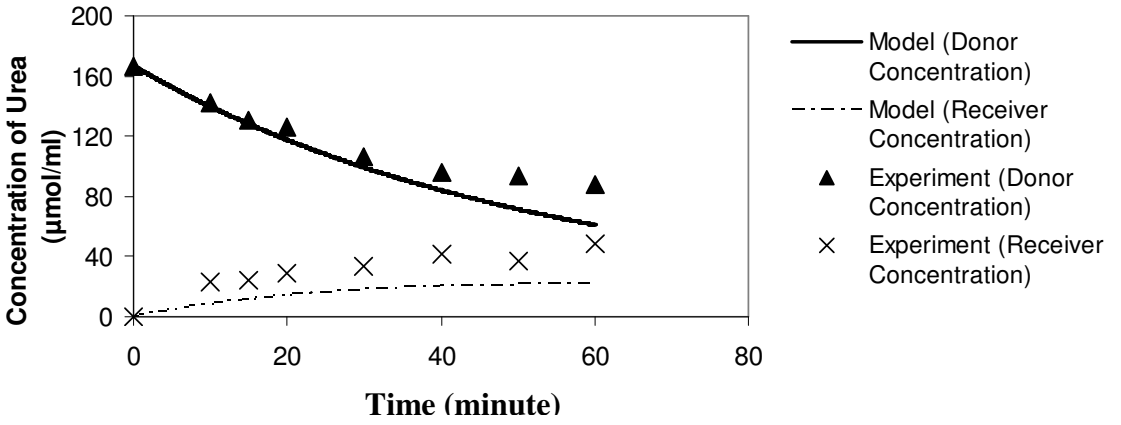

Figure 7.32. Comparison of model predictions with the experimental data for the concentration of urea in both donor and receiver compartments.

Figure 7.32 shows the comparison of model predictions and experimental data for the concentration of urea in the donor and receiver compartments, in the case of BSA fouled urease immobilized membrane. Except the diffusivity of urea in the

membrane, the same input data listed in Table 7.7. were used for model predictions. Diffusivity of urea in the BSA fouled urease immobilized CA membrane was regressed as 4.75×10^{-11} cm²/sec by minimizing the same objective function shown in Equation (7.2).

The agreement between model predictions and the experimental data for the urea concentration in the donor compartment is good until 40 minutes. The model predicts lower urea concentrations in the receiver compartment almost at all times. As discussed before, this is due to the combined effects of two factors which were not considered in the model: i) Inactivation of enzyme with time ii) Inhibition effect of products on the conversion of the urea.

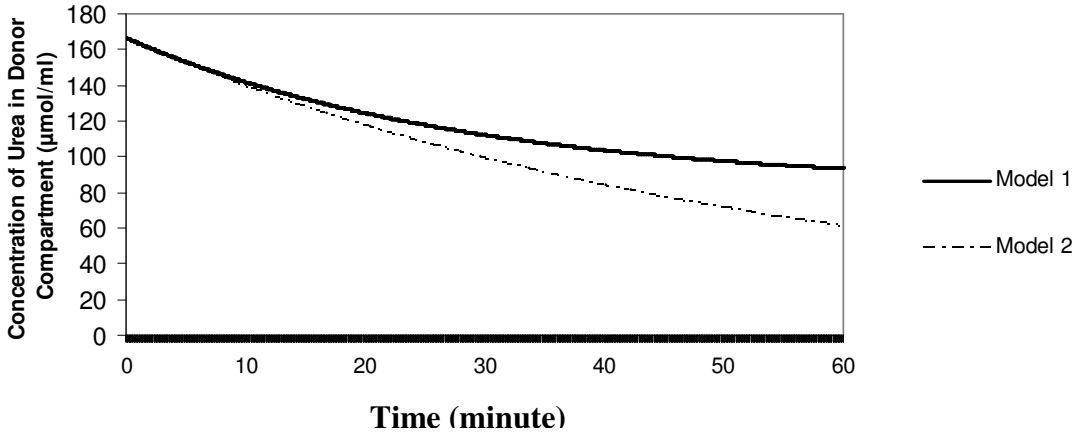

Figure 7.33. Predictions of concentration of urea in the donor compartment. Model 1 gives the urea concentration when BSA fouled regular CA membrane is used, while model 2 predicts the urea concentration when BSA fouled urease immobilized CA membrane is used.

Figure 7.33 shows the change in the urea concentration in the donor compartment when regular CA and urease immobilized CA membranes were used. The predictions are based on the average permeation coefficient of urea determined for the BSA fouled CA membrane (model 1) and the kinetic parameters listed in Table 7.7. and the diffusion coefficient of urea in the BSA fouled urease immobilized CA membrane (model 2). At short times, two models predict the same urea concentrations indicating that the transport of urea is governed by its diffusion in the membrane. Once the

diffusional resistance is overcomed, then model 2 predicts lower urea concentrations due to decomposition of urea by the urease enzyme.

7.5. Mechanical Properties of Cellulose Acetate Membranes

The stres-strain curves of the CA membranes prepared by changing CA/acetone weight percent ratio from 5/80 to 15/80 are shown in Figure 7.34 through Figure 7.37. The data shown in these figures correspond to the average of five independent measuements. Maximum tensile stress at the break point and Young's modulus calculated from the linear partion of the stres-strain curves are listed in Table 7.8.

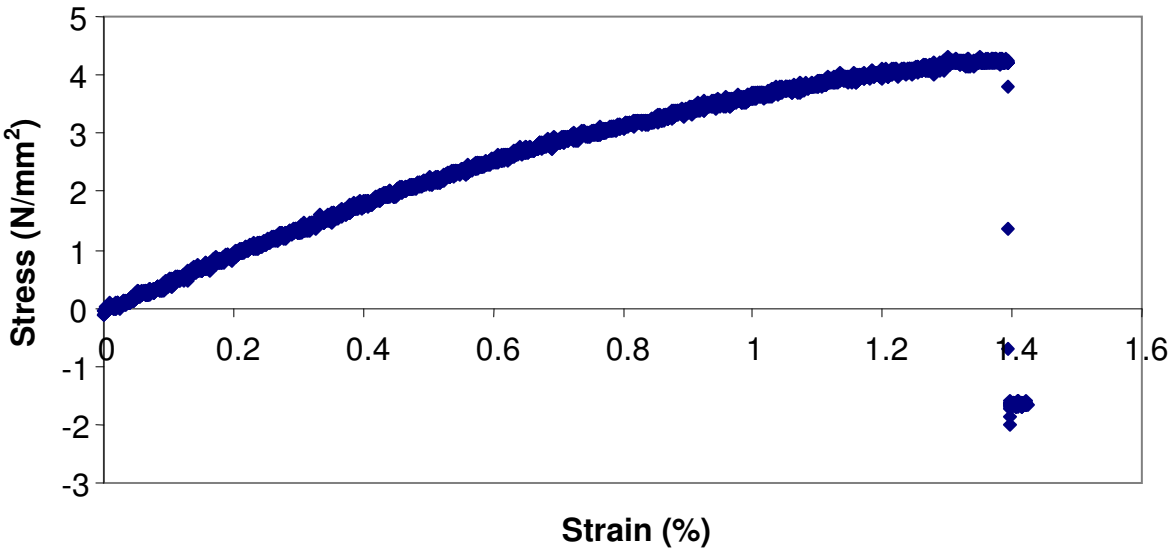

Figure 7.34 Stress vs. strain curve for CAI membrane.

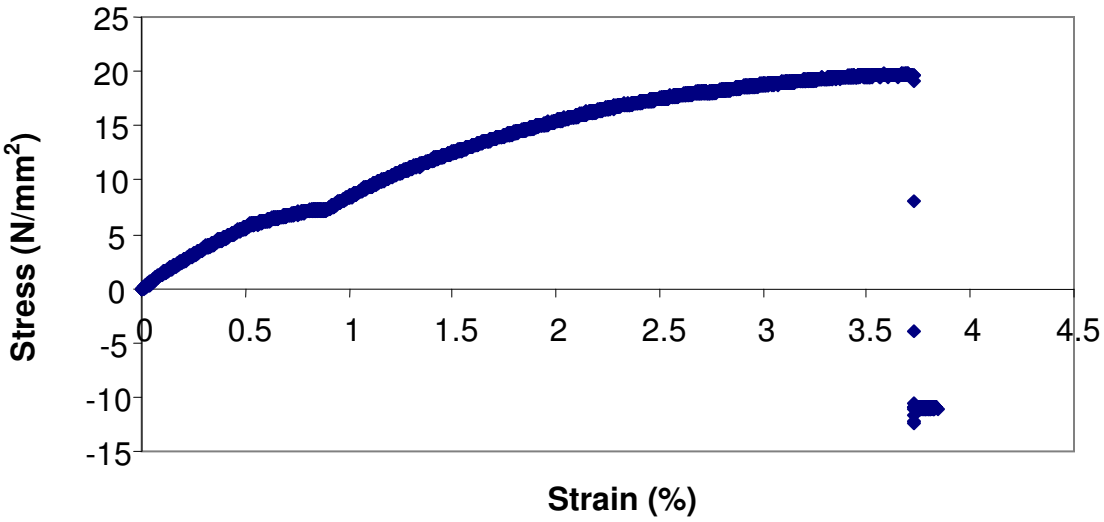

Figure 7.35. Stress vs. strain curve for CAII membrane.

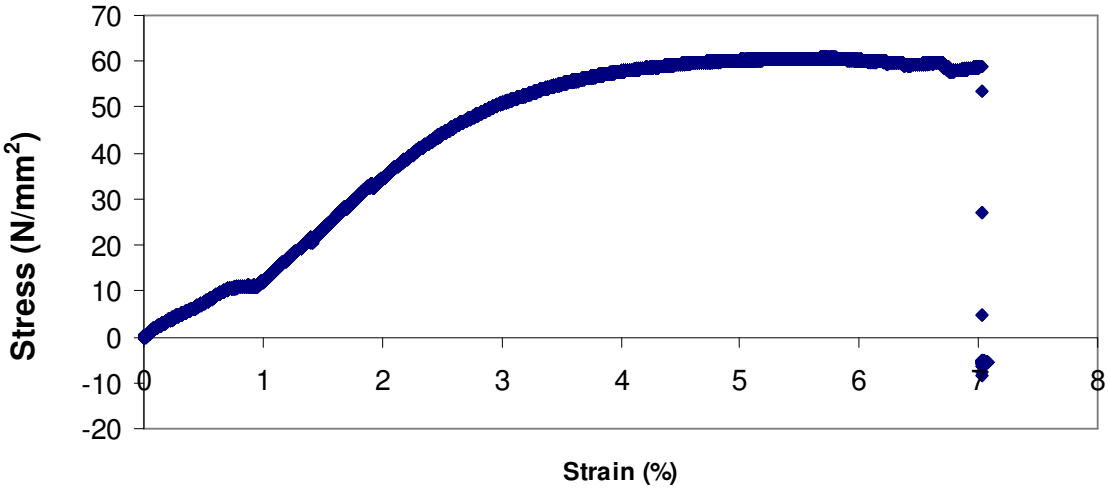

Figure 7.36. Sress vs. strain curve for CAIII membrane.

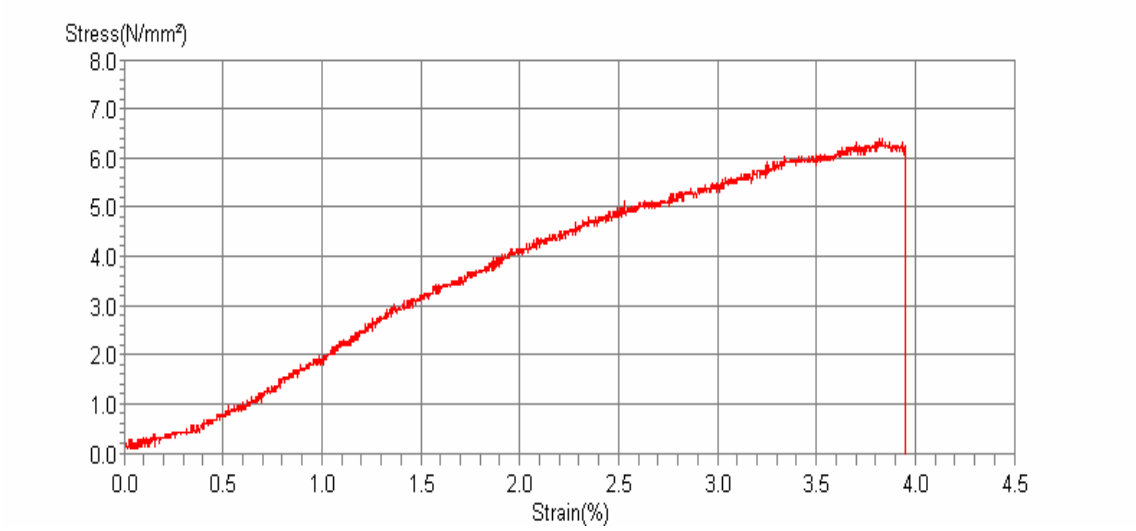

Figure 7.37. Stress vs. strain curve for urease immobilized CA membrane.

Table 7.8. Mechanical properties of CAI, CAII, CAIII and urease immobilized CA membranes.

Membrane		Maximum Tensile Stress (kN/m^2)	Young's Modulus (kN/m^2)
CAI	**Set 1**	3200	2210
	Set 2	4200	4120
	Set 3	4730	2980
	Set 4	4100	2020
	Set 5	2520	1510
	Average	**3750**	**2568**
	STD	**880**	**1016**
CAII	**Set 1**	10370	4820
	Set 2	19690	9120
	Set 3	22390	10290
	Set 4	24370	7450
	Set 5	20830	8050
	Average	**19530**	**7946**
	STD	**5414**	**2056**
CAIII	**Set 1**	61000	20210
	Set 2	60700	15650
	Set 3	55600	15600
	Set 4	47620	18600
	Set 5	68000	26700
	Average	**58584**	**19352**
	STD	**7551**	**4557**
Urease Immobilized CA Membrane	**Set 1**	6200	2000
	Set 2	7800	2670
	Set 3	7000	2500
	Set 4	4800	4000
	Set 5	7800	2500
	Average	**6720**	**2734**
	STD	**1262**	**751**

By increasing the CA concentration in the casting solution from 5% to 15%, maximum tensile strength and Young's Modulus increased 16 times and 8 times, respectively, due to a change in the structure of the membrane from porous to dense ones. The stress-strain curve for urease immobilized CA membrane is shown in Figure 7.37. The results in Table 7.8. indicate that by adding 0.5% urease into the casting solution containing 5% CA, the maximum tensile strength increased almost by a factor 2, while the Young's modulus remains approximately same. Increase in the tensile strength with the urease immobilization is mainly due to disappeareance of macrovoids and the blockage of some of the pores present in CAI membrane by the urease enzyme.

The mechanical properties of CA membranes prepared in this study were compared with those prepared by Ye et al. (2003) as shown in Table 7.9. To improve mechanical and transport properties, they have blended CA, with poly(2-methacryloyloxyethyl phosphorylcholine (MPC)-co-n-butyl methacrylate (BMA)(PMB30). The ratio of the composition of CA to PMB30 was kept constant and by changing the preparation conditions such as solvent evaporation time and the temperature of the coagulation bath three different blends were prepared. The maximum tensile strength of these membranes is similar to that of the CAI membrane prepared with 5% CA in the casting solution, while their Young's modulus are much higher than those of the all types of CA membranes prepared in this study.

Table 7.9. Maximum tensile stress of CA membranes.

Reference	Membranes	Maximum Tensile Stress (kN/m^2)	Young's Modulus (kN/m^2)	Membrane Thickness (μm)
This study	CAI	3750	2568	27.94
	CAII	19530	7946	19.69
	CAIII	58584	19352	19.16
	Urease Immobilized CA Membrane	6720	2734	16.71
S.H. Ye et al (2003)	Cellulose Acetate	2800	73000	82.00
	CA/PMB30 I*	2400	55000	87.00
	CA/PMB30 II*	3800	72000	81.00
	CA/PMB30 III*	3000	69000	85.00

* PMB30 :poly(2-methacryloyloxyethyl phosphorylcholine (MPC)-co-n-butyl methacrylate (BMA). Numbers represent the different preparation conditions.

CHAPTER 8

COCLUSIONS AND RECOMMENDATIONS FOR FUTURE WORK

In this study, asymmetric cellulose acetate membranes were prepared by dry-phase inversion method and they were modified through urease enzyme immobilization. The effect of cellulose acetate (CA) content in the initial casting solution on the permeabilities was examined with increasing the CA content in the solution. The permeation coefficients of all model solutes, uric acid, creatinine and urea, decreased exponentially since the average pore sizes decreased while the percentage of dense skin layer of the membrane increased. In addition, the permeation coefficients decreased exponentially with the increased molecular weight of the solute.

The urease immobilized CA membrane was characterized by first determining its stability in dry/wet conditions and kinetic parameters. 30% of the initial activity of immobilized urease was lost in 3 hours when CA membrane was stored at 37°C in a pH 7.4 phosphate buffer solution. On the other hand, dry-stored immobilized urease retained almost 85% of its initial activity for 60 days. Kinetic measurements indicated that decomposition of urea follows Michaelis-Menten kinetic expression and maximum reaction rate and the reciprocal of the Michaelis constant, $1/K_m$, of the immobilized urease decreased compared with those of native urease. The urease immobilized CA membrane showed improved transport rates for all solutes over the regular CA membrane. The mathematical model derived for enzyme immobilized membrane indicated that urease immobilization enhances the rate of removal of urea from the donor compartment especially at later stages of the experiment.

The protein adsorption capacity of the urease immobilized CA membrane was found to be lower than that of the regular CA membrane. Protein fouling caused a decline in the rate of transport of all solutes through both types of membranes. However, the decrease in the transport rates due to the protein fouling is lower for urease immobilized CA membrane.

The influences of polymer content in the casting solution and urease immobilization on the mechanical properties of the CA membranes were also investigated. With increased CA concentration in the solution, both the maximum

tensile stress and Young's Modulus increased significantly. The maximum tensile stress of the CA membrane was improved through urease immobilization due to disappearance of macrovoids.

In this study, enzyme immobilized hemodialysis membrane were prepared by directly blending urease enzyme into the casting solution. As a future work, it is recommended to use other immobilization techniques and investigate their effect on the stability of the enzyme. In addition, it is suggested to determine optimum enzyme immobilization conditions, such as pH, temperature, and enzyme concentration.

REFERENCES

Altinkaya, S.A., Ozbas, B. 2004. "Modeling of asymmetric membrane formation by dry-casting method", Journal of Membrane Science, Vol. 230, p. 71-89.

Altinkaya, S.A., Yenal, H., Ozbas, B. 2005. "Membrane formation by dry-cast process model validation through morphological studies", Journal of Membrane Science, Vol. 249, p. 163-172.

Babb, A.L., 1983 "Lymph filtration system" US Patent 4,411,792 (1983).

Bradford, M.M., 1976 "Analytical Biochemistry" 72, 248-254.

Brink, L.E.S., Elbers, S.J.G., Robbertsen, T., Both, P. 1993. "The anti-fouling action of polymers preadsorbed on ultrafiltration and microfiltration membranes", Journal Membrane Science., Vol. 76, p. 281.

Chen, V., Fane, A. G., Fell, C. J. D. 1992. "The use of anionic surfactants for reducing fouling of ultrafiltration membranes: their effects and optimization" Journal Membrane Science, Vol. 67, p. 249.

Clark, W. R., Gao, D. 2002. "Properties of Membranes Used for Hemodialysis Therapy", Seminars in Dialysis, Vol. 15, p. 191-195.

Dennis, M.B., Vizzo, J.E., Cole, J. J., Westendorf, D.L., Ahmad, S. 1986. "Comparison of four methods of cleaning hollow-fiber dialyzers for reuse" Artificial Organs, Vol. 10, p. 448.

Deppisch, R., Storr, M., Buck, R., Göhl, H. 1998. "Blood material interactions at the surfaces of membranes in medical applications", Separation and Purification Technology, Vol. 14, p. 241-254.

Giorno, L., Drioli, E. 2000. "Biocatalytic membrane reactors: applications and perspectives" Tibtech August, Vol. 18, p. 379.

Hargrove, S.C., Ilias, S., 2000 "Flux enhancement in cross flow membrane filtration by flow reversal: a case study on ultrafiltration of BSA, in: Proceedings of the IIChE Congress, CHEMCON 2000, Calcutta, India.

Hasegawa, T., Iwasaki, Y., Ishihara, K. 2001. "Preparation and performance of protein-adsorption-resistant asymmetric porous membrane composed of polysulfone /phospholipid polymer blend", Biomaterials, Vol. 22, p. 243-251.

Hayward, J.A., Chapman, D. 1984. "Biomembrane surfaces as models for polymer design: the potential for hemocompatibility" Biomaterials, Vol. 5, p. 135.

Higuchi, A., Iwata, N., Nakagawa, T. 1990. "Surface-modified polysulfone hollow fibers. II. Fibers having $CH_2CH_2CH_2SO_3$ segments and immersed in HCl solution", J. Appl. Polym. Sci., Vol. 40, p.709.

Higuchi, A., Nakagawa, T. 1990. " Surface-modified polysulfone hollow fibers. III. Fibers having a hydroxide group", J. Appl. Polym. Sci., Vol.41, p.1973.

Ishihara, K., Ueda, T., Nakabayashi, N. 1990. "Preparation of phospholipid polymers and their properties as polymer hydrogel membranes", Polym. J. Vol. 22, p.355.

Ilias, S., Hargrove, S.C., Talbert, M.E. 2001 "Flux-enhanced crossflow membrane fitler" US Patent 6,168,714 (2001).

Hester, J. F., Mayes, A.M. 2002. "Design and performance of foul-resistant poly(vinylidene fluoride) membranes prepared in a single-step by surface segregation", J. Membr. Sci., Vol. 202, p. 119.

Krajewska, B., Lezko, M., Zaborska, W. 1990. "Urease immobilized on chitosan membrane: preparation and properties", J.Chem Technol Biotechnol., Vol. 48, p. 337-350.

Li, D., Krantz, W.B., Greenberg, A.R., Sani, R.L. 2006. "Membrane formation via thermally induced phase separation (TIPS): Model development and validation", Journal of Membrane Science, Vol. 279, p. 50-60.

Lin, C. C., Liu, T. Y., Yang, M. C. 2004. "Hemocompatibility of polyacrylonitrile dialysis membrane immobilized with chitosan and heparin conjugate" ,Biomaterials, Vol. 25, p. 1947-1957.

Lin,C.C., Yang, M.C., 2003. "Urea permeation and hydrolysis through hollow fiber dialyzer immobilized with urease: storage and operation properties", Biomaterials, Vol. 24, p.1998-1994.

Mok, S., Worsfold, D.J., Fouda, A., Matsuura, T. 1994. "Surface modification of polyethersulfone hollow-fiber membranes by -ray irradiation" J. Appl. Polym. Sci., Vol. 51, p. 193.

Morti, S., Shao, J., Zydney, A. L. 2003. "Importance of asymmetric structure in determining mass transport characteristics of hollow fiber hemodialyzers", Journal of Membrane Science, Vol. 224, p. 39.

Nie, F. Q., Xu, Z. K., Ye, P., Wu, J., Seta, P. 2004. "Acrylonitrile-based copolymer membranes containing reactive groups: effects of surface-immobilized poly(ethylene glycol)s on anti-fouling properties and blood compatibility" Polymer, Vol. 45, p. 399-407.

Penky, M. R., Greenberg, A. R., Khare, V., Zartman, J., Krantz, W. B., Todd, P. 2002. "Macrovoid pore formation in dry-cast cellulose acetate membranes: buoyancy studies", Journal of Membrane Science, Vol. 205, p. 11-21.

Penky, M. R., Zartman, J., Krantz, W. B., Greenberg, A. R., Todd, P. 2003. "Flow-visualization during macrovoid pore formation in dry-cast cellulose acetate membranes", Journal of Membrane Science, Vol. 205, p. 71-90.

Ruthven, D. M. "Encyclopedia of Separation Technology", John Wiley & Sons, 1997.

Saltürk, A. G. D. 2006. "Hemodiyaliz Hastalarında Yaşam Kalitesinin Diyaliz Yeterliliği İle İlişkisi" Uzmanlık Tezi, T.C. Sağlık Bakanlığı İstanbul Göztepe Eğitim ve Araştırma Hastanesi, İstanbul.

Seita, Y., Mochizuki, A., Nakagawa, M., Takanashi, K., Yamashita, S. 1997 "Polyether-Segmented nylon Hemodialysis Membrane. I. Preparation and permeability characteristics of Polyether-Segment Nylon 610 Hemodialysis Membrane, John Wiley & Sons, p 1703-1711

Stropnik, C., Kaiser, V. 2002. " Polymeric membranes preparation by wet phase separation: mechanisms and elementary processes", Desalination, Vol. 145, p. 1.

Tsai, H.A., Lin, J.H., Wang, D.M., Lee, K.R., Lai, J.Y. 2006. "Effect of vapor-induced phase separation on the morphology and separation performance of polysulfone hollow fiber membranes", Desalination, Vol. 200, p. 247-249.

Ulbricht, M., Matuschewski, H., Oechel, A., Hicke, H.-G. 1996. "Photo-induced graft polymerization surface modifications for the preparation of hydrophilic and low protein-adsorbing ultrafiltration membranes", J. Membr. Sci., Vol. 115, p. 31.

Uragami, T., Ueguchi, K., Watanabe, M., Miyata, T. 2006. "Preparation of urease – immobilized polymeric membranes and their function", Catalysis Today, Vol. 118, p.158-165.

Wang, Y., Kim, J.H., Choo, K.-H., Lee, Y.S., Lee, C.H. 2000. "Hydrophilic modification of polypropylene microfiltration membranes by ozone-induced graft polymerization", J.Membr. Sci., Vol. 169, p. 269.

Ward, R.A., Klein, E., Harding, G.B., Murchison, K.E. 1998. "Response of complement and neutrophils to hydrophilized synthetic membranes" Trans. Am. Soc. Artif. Intern. Organs. Vol. 34, p. 334.

Weatherburn, M. W. 1967. "Phenol-Hypochlorite Reaction for Determination of Ammonia", Laborotary of Hygiene, National Health and Welfare, Vol. 39, p. 971-974.

WEB_1 National Kidney and Urologic Diseases Information Clearinghouse www.kidney.niddk.nih.gov/kudiseases/pubs/kidneyfailure/index.htm (13.12.2006)

Woffinfin, C., Hoenich, N.A. 1988. "Blood-membrane interactions during haemodialysis with cellulose and synthetic membranes", Biomaterials, Vol. 9, p. 53.

Yang, M.C., Lin, C.C. 2001. “Urea permeation and hydrolysis through hollow fiber dialyzer immobilized with urease”, Biomaterials, Vol. 22, p. 891-896.

Yang, M. C., Liu, T. Y. 2003. “The Permeation Performance of Polyacrylonitrile/ polyvinylidine Fluoride blend Membranes”, Journal of membrane Science, Vol. 226, p. 119-130.

Ye, S.H., Watanabe ,J., Iwasaki ,Y., Ishihara, K. 2002. “Novel cellulose acetate membrane blended with phospholipid polymer for hemocompatible filtration system”, Journal of Membrane Science, Vol. 210, p. 411-421.

Ye, S. H., Watanabe, J., Iwasaki, Y., Ishihara, K. 2005. “In situ modification on cellulose acetate hollow fiber membrane modified with phospholipid polymer for biomedical application”, Journal of Membrane Science, Vol. 249, p. 133-141.

Ye, S. H., Watanabe, J., Iwasaki, Y., Ishihara, K. 2003. “Antifouling blood purification membrane composed of cellulose acetate and phospholipid polymer”, Biomaterials, Vol. 24, p. 4143-4152.

Yin, G. J., Janson, C., Liu, Z. 2000. “Characterization of protein adsorption on membrane surface by enzyme linked immunoassay”, J. Membr. Sci., Vol. 178, p. 99.

Yip, Y., McHugh, A.J. 2006. “Modeling and simulation of nonsolvent vapor-induced phase separation” Journal of Membrane Science, Vol. 271, p.163-176.

APPENDIX A

CALIBRATION CURVES

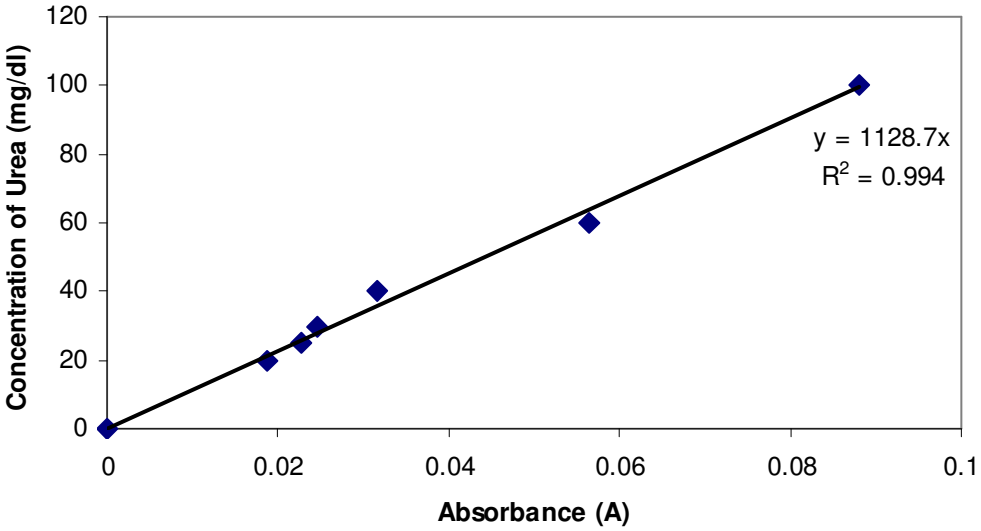

Figure A. 1. Calibration curve for urea.

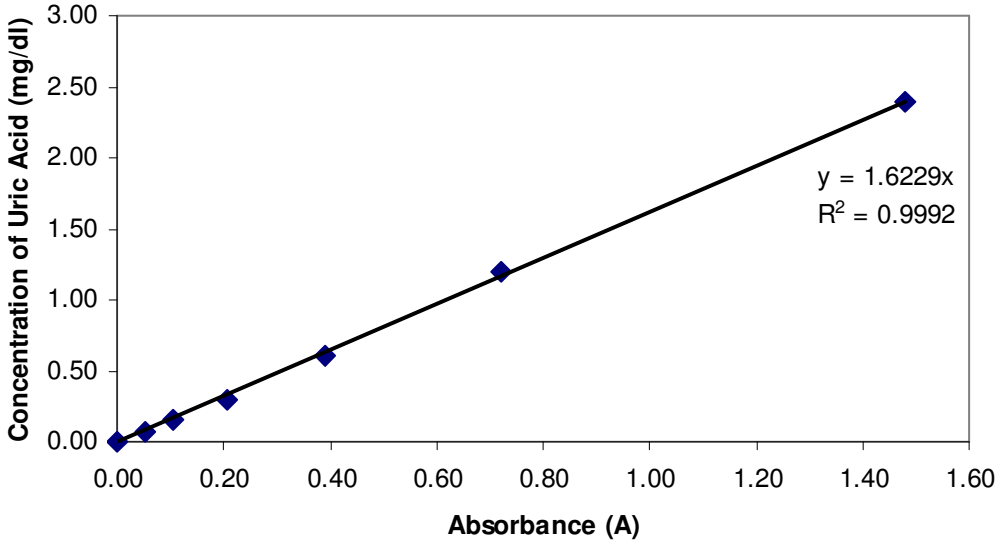

Figure A. 2. Calibration curve for uric acid.

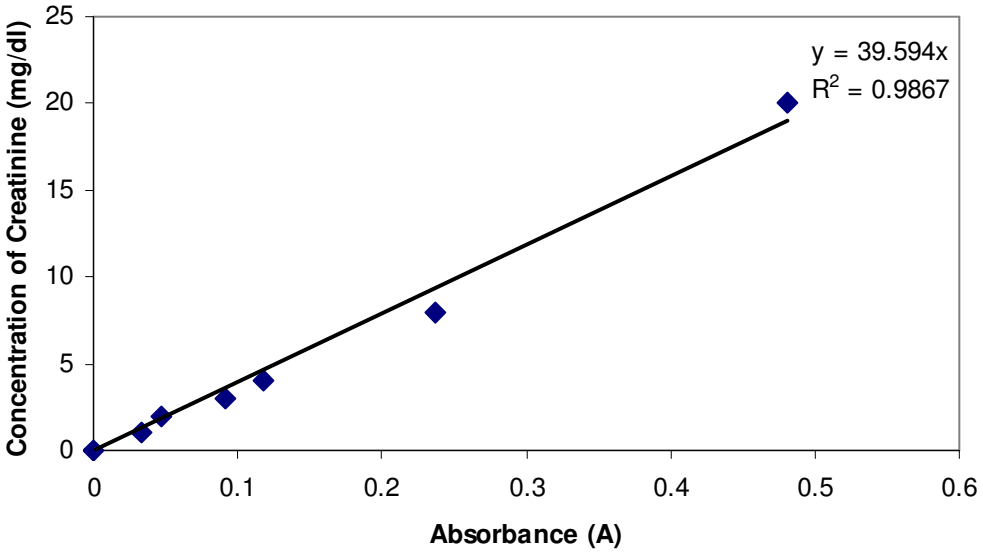

Figure A. 3. Calibration curve for Creatinine.

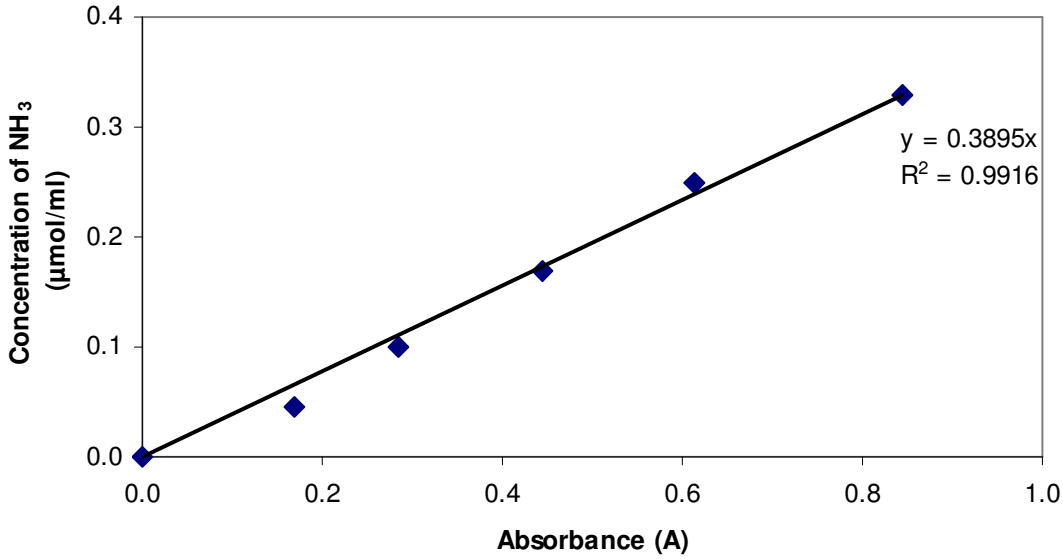

Figure A. 4. Calibration curve for NH_3.